

**INVESTIGATION ON THE GOLD NANOPARTICLES  
CONCENTRATION EFFECTS TO THE OPTICAL AND  
STRUCTURAL PROPERTIES OF NANOSTRUCTURE  
GLASS**

**REUBEN HO CHEE WUI**

**PERPUSTAKAAN  
UNIVERSITI MALAYSIA SABAH**

**THESIS SUBMITTED IN FULFILLMENT OF THE  
REQUIREMENTS FOR THE DEGREE OF MASTER OF  
SCIENCE**

**FACULTY OF SCIENCE AND NATURAL RESOURCES  
UNIVERSITI MALAYSIA SABAH  
2019**



**UMS**  
UNIVERSITI MALAYSIA SABAH

UNIVERSITI MALAYSIA SABAH

BORANG PENGESAHAN TESIS

JUDUL: **INVESTIGATION ON THE GOLD NANOPARTICLES CONCENTRATION EFFECTS TO THE OPTICAL AND STRUCTURAL PROPERTIES OF NANOSTRUCTURE GLASS**

IJAZAH: **SARJANA SAINS (FIZIK DENGAN ELEKTRONIK)**

Saya **REUBEN HO CHEE WUI**, sesi **2014-2019**, mengaku membenarkan tesis Sarjana ini disimpan di Perpustakaan Universiti Malaysia Sabah dengan syarat-syarat kegunaan seperti berikut:

1. Tesis ini adalah hak milik Universiti Malaysia Sabah.
2. Perpustakaan Universiti Malaysia Sabah dibenarkan membuat salinan untuk tujuan pengajian sahaja.
3. Perpustakaan dibenarkan membuat salinan tesis ini sebagai bahan pertukaran antara institusi pengajian tinggi.
4. Sila tandakan (/):

SULIT

(Mengandungi maklumat yang berdarjah keselamatan atau kepegeangan, Malaysia seperti yang termaktub di dalam AKTA RAHSIA 1972)

TERHAD

(Mengandungi maklumat TERHAD yang telah ditentukan oleh organisasi/badan di mana penyelidikan dijalankan)

TIDAK TERHAD

**REUBEN HO CHEE WUI**  
**MS1421113T**

Tarikh: 9 JULAI 2019

NORAZDYNNORAHMAN@J.K.MYNE  
PUSTAKAWAN  
UNIVERSITI MALAYSIA SABAH  
(Tanda Tangan Pustakawan)

10.7.2019

Prof. Madya Dr. Jedol Dayou  
Pengerusi J/K Penyeliaan

**Prof. Madya Dr. Jedol Dayou**  
Program Fizik Dengan Elektronik  
Fakulti Sains dan Sumber Alam  
UNIVERSITI MALAYSIA SABAH



**UMS**  
UNIVERSITI MALAYSIA SABAH

PERPUSTAKAAN  
UNIVERSITI MALAYSIA SABAH

## DECLARATION

I hereby declare that the work in this thesis is my own except for quotation, equations, summaries and references which have been acknowledged.

9 July 2019

*Reuben*

---

Reuben Ho Chee Wui

MS1421113T

## CERTIFICATION

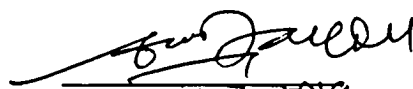
NAME : REUBEN HO CHEE WUI  
MATRIC NO. : MS1421113T  
TITLE : INVESTIGATION ON THE GOLD NANOPARTICLES  
CONCENTRATION EFFECTS TO THE OPTICAL AND  
STRUCTURAL PROPERTIES OF NANOSTRUCTURE GLASS  
DEGREE : MASTER OF SCIENCE (PHYSICS WITH ELECTRONICS)  
VIVA DATE : 9 APRIL 2019

### CERTIFIED BY:

**1. CHAIRPERSON OF RESEARCH COMMITTEE**

Assoc. Prof. Dr. Jedol Dayou

Signature

  
10.7.2019  
**Prof. Madya Dr. Jedol Dayou**  
Program Fizik Dengan Elektronik  
Fakulti Sains dan Sumber Alam  
UNIVERSITI MALAYSIA SABAH

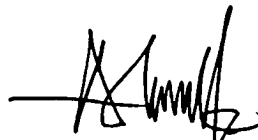
**2. MEMBER OF RESEARCH COMMITTEE 1**

Dr. Asmahani Awang

  
\_\_\_\_\_

**3. MEMBER OF RESEARCH COMMITTEE 2**

Dr. Alvie Lo Sin Voi

  
\_\_\_\_\_

PERPUSTAKAAN  
UNIVERSITI MALAYSIA SABAH



## **ACKNOWLEDGEMENT**

A special gratitude to my chairperson (Assoc. Prof. Dr. Jedol Dayou) and members (Dr. Asmahani Awang and Dr. Alvie Lo Sin Voi) of the research committee who helped and guided me during the period of this research. Their guidance, idea and constructive comments helped me to coordinate my research and finally complete my thesis.

Last but not least, I would like to thank my fellow lab mates (e-vibs, Makmal Bahan Kimia Semula Jadi and Makmal Bahan Sains) for ideas and encouragement during the period of my research.

Reuben Ho Chee Wui

9 July 2019



## ABSTRACT

Achieving enhancement of photoluminescence and Raman spectra of glasses containing rare-earth ions and metallic nanoparticles are prerequisite. Many studies only reported the effect of concentration of the nanoparticles on structural and optical properties of the glasses instead of the variation in size and shape of nanoparticles. Thus, the current study aims to investigate effect of concentration of the gold (Au) nanoparticles on structural and optical properties of the glasses. Further, their geometric effect on photoluminescence and Raman enhancement with varying concentration of the gold nanoparticles for optimizing photoluminescence and Raman enhancement are addressed. A series of glass with composition of  $70\text{TeO}_2\text{-}20\text{ZnO}\text{-}10\text{Na}_2\text{O}\text{-}0.5\text{Er}_2\text{O}_3\text{-}(x)\text{Au}$  where  $x=0.0, 0.1, 0.2, 0.3$  and  $0.4$  mol% were examined with X-ray diffraction (XRD), ultraviolet-visible (UV-Vis) spectroscopy, transmission electron microscopy (TEM), scanning electron microscopy (SEM), energy dispersive X-ray spectroscopy (EDX), photoluminescence spectroscopy, Fourier Transform Infrared (FTIR) spectroscopy and Raman spectroscopy. Modification in UV-Vis spectra was observed due to non-bridging oxygen created by gold nanoparticles with increasing concentration of gold nanoparticles. TEM images verified the presence of non-spherical gold nanoparticles. Photoluminescence spectra revealed luminescence enhancement caused by the effect of surface plasmon resonance (SPR) and energy transfer from the gold nanoparticles to erbium ions as concentration of the gold nanoparticles was increased up to 0.3 mol%. However, when the concentration of the gold nanoparticles exceeded 0.3 mol%, luminescence quenching occurs due to energy transfer from erbium ions to gold nanoparticles. Amplification of Raman spectra was attributed to the effect of SPR. The concentrations of the gold nanoparticles for maximizing photoluminescence and Raman spectra were found to be 0.3 and 0.4 mol%, respectively. Non-spherical shaped nanoparticles were found to optimize photoluminescence and Raman enhancement. The results demonstrated the effect of varying concentration of nanoparticles on the properties of the glasses due to the geometric effect of the nanoparticles especially on the enhancement of photoluminescence and Raman spectra.

## ABSTRAK

### **KAJIAN KESAN KEPEKATAN ZARAH NANO EMAS TERHADAP SIFAT OPTIK DAN STRUKTUR BAGI KACA BERSTRUKTUR NANO**

*Peningkatan spektra fotoluminesen dan Raman bagi kaca yang mengandungi ion-ion bumi nadir dan zarah nano logam adalah sangat penting. Kebanyakan kajian hanya melaporkan pengaruh kepekatan zarah nano terhadap sifat-sifat struktur dan optik kaca tersebut tetapi tidak melaporkan kepelbagaian pada saiz dan bentuk zarah nano. Maka, kajian ini bertujuan untuk mengkaji kesan kepekatan zarah nano emas pada sifat struktur dan optik kaca. Tambahan pula, kesan geometri pada peningkatan fotoluminesen dan Raman dengan kepelbagaian zarah nano emas untuk mendapatkan peningkatan fotoluminesen dan Raman yang optimum dibincangkan. Satu siri kaca yang mempunyai komposisi  $70\text{TeO}_2\text{-}20\text{ZnO}\text{-}10\text{Na}_2\text{O}\text{-}0.5\text{Er}_2\text{O}_3\text{-}(x)\text{Au}$  di mana  $x=0.0, 0.1, 0.2, 0.3$  dan  $0.4$  mol% telah dikaji menggunakan teknik pembelauan sinar-X (XRD), spektroskopi ultraungu-cahaya nampak (UV-Vis), mikroskopi pancaran elektron (TEM), mikroskopi pengimbasan elektron (SEM), spektroskopi serakan tenaga sinar-X (EDX), spektroskopi fotoluminesen, spektroskopi Inframerah Pengubah Fourier (FTIR) dan spektroskopi Raman. Perubahan pada spektrum UV-Vis disebabkan oleh ikatan oksigen tidak bersambung yang dihasilkan oleh zarah nano emas apabila kepekatan zarah nano emas ditingkatkan. Imej TEM membuktikan kehadiran zarah nano emas yang mempunyai bentuk bukan sfera. Spektrum fotoluminesen menunjukkan peningkatan daripada kesan resonan plasmon permukaan (SPR) dan pemindahan tenaga daripada zarah nano emas kepada ion-ion erbiium apabila kepekatan zarah nano emas ditingkatkan sehingga  $0.3$  mol%. Bagaimanapun, apabila kepekatan zarah nano emas melebihi  $0.3$  mol%, penurunan pada keamatan fotoluminesen berlaku disebabkan pemindahan tenaga daripada ion-ion erbiium kepada zarah nano emas. Peningkatan spektrum Raman disebabkan oleh kesan SPR. Didapati kepekatan zarah nano emas untuk mengoptimumkan peningkatan fotoluminesen dan Raman ialah  $0.3$  dan  $0.4$  mol%. Zarah nano berbentuk bukan sfera mengoptimumkan peningkatan fotoluminesen dan Raman. Keputusan tersebut menunjukkan kesan kepekatan zarah nano terhadap sifat-sifat kaca disebabkan kesan geometri terutamanya pada peningkatan spektra fotoluminesen dan Raman.*



## TABLE OF CONTENTS

	Page
<b>TITLE</b>	i
<b>DECLARATION</b>	ii
<b>CERTIFICATION</b>	iii
<b>ACKNOWLEDGEMENT</b>	iv
<b>ABSTRACT</b>	v
<b><i>ABSTRAK</i></b>	vi
<b>TABLE OF CONTENTS</b>	vii
<b>LIST OF TABLES</b>	x
<b>LIST OF FIGURES</b>	xi
<b>LIST OF ABBREVIATIONS AND SYMBOLS</b>	xvii
<b>LIST OF APPENDICES</b>	xxi
<b>CHAPTER 1 : INTRODUCTION</b>	
1.1 Overview of the Study	1
1.2 Research Problem	3
1.3 Research Objectives	4
1.4 Scope of Study	4
1.5 Research Limitation	5
<b>CHAPTER 2 : LITERATURE REVIEW</b>	
2.1 Introduction	6
2.2 Glass	7
2.2.1 Definition of Glass and Amorphous Solids	7





2.2.2	Structural Properties of Glass	8
2.2.3	Tellurite Glass	10
2.3	Glass Modifiers	12
2.4	Rare Earth Ions	14
2.5	Metallic Nanoparticles and Advantages of Glasses as Encapsulating Hosts	16
2.6	Aspect Ratio	20
2.7	Surface Plasmon and Surface Plasmon Resonance (SPR)	20
2.8	Band Gaps	23
2.9	Urbach Energy	25
2.10	Physical Principles of Experimental Techniques	26
2.10.1	X-ray Diffraction (XRD)	26
2.10.2	UV-Vis Spectroscopy	28
2.10.3	Photoluminescence Spectroscopy	29
2.10.4	Fourier Transform Infrared Spectroscopy (FTIR)	31
2.10.5	Raman Spectroscopy	33
2.10.6	Transmission Electron Microscopy (TEM)	35
2.10.7	Scanning Electron Microscopy (SEM)	36
2.10.8	Energy Dispersive X-ray Spectroscopy (EDX)	37

### **CHAPTER 3 : METHODOLOGY**

3.1	Introduction	39
3.2	Sample Preparation	41
3.3	Sample Cutting Process	42
3.4	Sample Polishing Process	43
3.5	Sample Cleaning Process	45
3.6	Sample Characterization	45
3.6.1	X-Ray Diffraction (XRD)	45

3.6.2	UV-Vis Spectroscopy	47
3.6.3	Photoluminescence Spectroscopy	51
3.6.4	Fourier Transform Infrared Spectroscopy (FTIR)	56
3.6.5	Raman Spectroscopy	59
3.6.6	Transmission Electron Microscopy (TEM)	62
3.6.7	Scanning Electron Microscopy (SEM)	64
3.6.8	Energy Dispersive X-Ray Spectroscopy (EDX)	67
<b>CHAPTER 4 : RESULTS AND DISCUSSIONS</b>		
4.1	Introduction	70
4.2	Structural Characterization	70
4.3	UV-Vis Spectroscopy	73
4.4	Transmission Electron Microscopy (TEM)	80
4.5	Scanning Electron Microscopy (SEM)	86
4.6	Energy Dispersive X-ray Spectroscopy (EDX)	87
4.7	Photoluminescence Spectroscopy	90
4.8	Fourier Transform Infrared Spectroscopy (FTIR)	100
4.9	Raman Spectroscopy	103
4.10	Summarization	107
<b>CHAPTER 5 : CONCLUSION</b>		
5.1	Conclusion	110
5.2	Future Outlook	112
<b>REFERENCES</b>		113
<b>APPENDICES</b>		134

## LIST OF TABLES

	Page
Table 2.1: Values of $n$ , and the types of optical transition that can occur in the material.	25
Table 3.1: Glass samples and their corresponding compositions and glass codes.	41
Table 4.1: Information about XRD peak and type of NPs in both samples.	72
Table 4.2: Positions of UV-Vis absorption peaks and their corresponding transitions of $\text{Er}^{3+}$ ions from ground state to excited states.	74
Table 4.3: Direct optical band gap ( $E_{dir}$ , eV), indirect optical band gap ( $E_{indir}$ , eV) and Urbach energy ( $E_U$ , eV) of glass samples with different concentration of the Au NPs.	75
Table 4.4: Variation of range of longitudinal axis, range of transverse axis, and mean aspect ratio of the Au NPs with increasing concentration of the Au NPs.	83
Table 4.5: Effect of increasing the concentration of the Au NPs on estimated size and standard deviation of the Au NPs.	86
Table 4.6: Excitation peaks and their corresponding transitions of $\text{Er}^{3+}$ ion from ground state to excited energy levels.	90
Table 4.7: Emission peaks and their corresponding peak labels, peak positions, transitions of $\text{Er}^{3+}$ ion from an excited state to the ground state, and corresponding references.	91
Table 4.8: Photoluminescence enhancement factor and concentration of Au NPs.	95
Table 4.9: IR peaks and their corresponding IR peak assignment	102
Table 4.10: Raman bands and their corresponding Raman band assignments.	105
Table 4.11: Change of FWHM of Raman spectrum with increasing Au concentration.	106

## LIST OF FIGURES

	Page
Figure 2.1: (a) Orderly arrangement of a crystalline solid (crystalline silica); (b) random arrangement of particles in an amorphous solid (silica glass).	7
Figure 2.2: Intensity distribution of X-ray diffraction pattern of: cristobalite (crystalline form of silicon dioxide) (top); and silica glass (amorphous form of silicon dioxide).	8
Figure 2.3: Volume against temperature (in Kelvin) showing liquid, crystalline and glass states of a glass.	9
Figure 2.4: Schematic diagram of $\text{TeO}_2$ unit in the structure of $\alpha\text{-TeO}_2$ .	10
Figure 2.5: $\text{TeO}_4$ tbp, $\text{TeO}_{3+1}$ and $\text{TeO}_3$ tp units of tellurite glass.	11
Figure 2.6: A flow chart illustrating preparation of glasses by melt-quenching technique.	18
Figure 2.7: Schematic diagram of Ostwald ripening process.	19
Figure 2.8: Simplified classical pictures of interaction between incident electromagnetic field and surface plasmons of gold NPs.	21
Figure 2.9: Schematic diagram of interaction between metallic NPs through field of different polarizations for (a) the first five metallic NPs interacting with each other is for transverse modes (b) the last five metallic NPs interacting with each other is for longitudinal modes.	23
Figure 2.10: An illustration of (a) a direct transition and (b) an indirect transition.	24
Figure 2.11: X-ray diffraction.	27
Figure 2.12: Absorption spectrum and energy level of $\text{Er}^{3+}$ ion in glass.	29
Figure 2.13: (a) Excitation spectra; (b) emission spectra of $\text{Er}^{3+}$ ions in Ge-Ga-S glass without silver NPs (shown by a black line and the label (a)) and the same type of glass with silver NPs	30

(shown by a blue line and the label (b)) as examples.

- Figure 2.14: Partial energy level diagram of  $\text{Er}^{3+}$  ion in tungstate-tellurite glasses as an example. 31
- Figure 2.15: An evanescent wave and how attenuated total reflection (ATR) occurs. 32
- Figure 2.16: A schematic diagram of Rayleigh and Raman scattering of electromagnetic wave from matter where  $\omega_1$  is angular frequency of the incident electromagnetic wave while  $\omega_M$  is shift of frequency after Raman scattering. 34
- Figure 2.17: Rayleigh and Raman spectra of carbon tetrachloride (liquid). 34
- Figure 2.18: Characteristic X-rays are emitted upon bombardment of an incident electron beam with an electron in an electron shell and subsequent ejection of the electron from electron shell. 38
- Figure 3.1: A flow chart summarizing the methodology of the current study. 40
- Figure 3.2: Glass samples and their corresponding labels based on their glass composition. 42
- Figure 3.3: Glass cutter. 43
- Figure 3.4: (a) Lam Plan 410 polishing pad; (b) Hyprez OS Type IV lubricant; (c) Hyprez Five Star 1  $\mu\text{m}$  (blue), 3  $\mu\text{m}$  (green) and 6  $\mu\text{m}$  (yellow) diamond polishing paste. Blue, green and yellow diamond polishing paste are at bottom right, upper left and bottom left of Figure 3.3 (c) respectively. 44
- Figure 3.5: A schematic diagram of X-ray diffractometer. 46
- Figure 3.6: Philips X'Pert Pro X-ray diffractometer. 47
- Figure 3.7: A schematic diagram of operation of UV-Vis spectrophotometer shows (a) a single-beam UV-Vis spectrophotometer; (b) a double-beam UV-Vis spectrophotometer. 48
- Figure 3.8: (a) Sample holders for each sample; (b) preparation of a sample holder with a label (S1 for an instance) to hold its 50

corresponding glass sample (TZNE0.5 for an example) before characterization of the glass sample by using the UV-Vis spectroscopy.

- Figure 3.9: (a) Agilent Technologies Cary 60 UV-Vis spectrophotometer; (b) internal structure of Agilent Technologies Cary 60 UV-Vis spectrophotometer. The hole to the sample detector is shown by a yellow oval mark. 50
- Figure 3.10: Demonstration of putting a sample holder sandwiching a glass sample before the use the UV-Vis spectrophotometer. The exposed part of the glass sample that is covering the hole to a sample detector is shown by a yellow oval mark while the holt where an incident light beam is indicated by a blue oval mark. 51
- Figure 3.11: A schematic diagram of photoluminescence spectroscopy. 52
- Figure 3.12: (a) Agilent Technologies Cary Eclipse fluorescence spectrophotometer; (b) internal structure of Cary Eclipse fluorescence spectrophotometer. 54
- Figure 3.13: (a) Illustration of inserting a glass sample labelled with S1 for TZNE0.5 into a sample holder as an example; (b) insertion of the sample holder containing the glass sample into a left hole of a cuvette holder inside the sample compartment before the use of the photoluminescence spectrophotometer. 55
- Figure 3.14: A schematic diagram of Michelson interferometer that is part of FTIR. 56
- Figure 3.15: Operation of ATR-FTIR. It shows an ATR crystal, and pressure being applied to a solid sample with a clamp for good sample/hot spot contact. 57
- Figure 3.16: (a) Perkin Elmer Spectrum 100 FTIR spectrometer; (b) an ATR accessory (shown by a yellow oval mark); (c) structure of the ATR accessory and analysis of powdered glass sample (shown by another yellow oval mark) on an ATR diamond inside the ATR accessory. 58
- Figure 3.17: Operation of ASEQ Raman spectrometer. 59
- Figure 3.18: ASEQ Raman spectrometer. 61

Figure 3.19: (a) View of a sample chamber of ASEQ Raman spectrometer when the cover of the sample chamber was turned up; (b) a glass sample labelled with S1 for TZNE0.5 that was inserted into a sample holder before its characterization with Raman spectroscopy.	61
Figure 3.20: A schematic diagram of the structure of a transmission electron microscope.	62
Figure 3.21: (a) TEM with a model called Fei Tecnai Spirit at IPB of UMS; (b) ultrasonic bath used for sample preparation for TEM for current study; (c) 300-mesh copper grid with carbon film.	64
Figure 3.22: A schematic diagram of a scanning electron microscope.	65
Figure 3.23: FEI Quanta FEG 650 scanning electron microscope (SEM).	66
Figure 3.24: Quorum Q150T at USM for coating a glass sample with carbon via vacuum-evaporation method.	66
Figure 3.25: A schematic diagram of an EDX detector and its detection process.	68
Figure 3.26: Oxford instrument X-Max 50 mm <sup>2</sup> silicon drift detector (SDD) attached to FEI Quanta FEG 650 scanning electron microscope (SEM) at Makmal Pencirian Bahan Bumi (MPBB) of Universiti Sains Malaysia (USM). This figure is an example of Oxford instrument X-Max SDD which comes with 3 different areas (30, 50 or 80 mm <sup>2</sup> ) as taken from brochures about X-Max SDD.	69
Figure 4.1: X-ray diffraction pattern of glass samples.	71
Figure 4.2: A diagram showing estimation of FWHM of an XRD peak due to Au NPs in TZNE0.5-Au 0.4 as an example.	73
Figure 4.3: UV-Vis absorption spectra of glass samples.	74
Figure 4.4: (a) Tauc plot for determining direct optical band gap of glass samples; (b) illustration to calculating direct optical band gap of TZNE0.5 sample as an example after drawing a straight line from the linear part the graph of the sample.	76

Figure 4.5:	(a) Tauc plot for determining indirect optical band gap of glass samples; (b) illustration to calculating indirect optical band gap of TZNE0.5 sample as an example after drawing a straight line from the linear part the graph of the sample.	76
Figure 4.6:	A graph of direct optical band gap versus concentration of Au NPs.	77
Figure 4.7:	A graph of indirect optical band gap versus concentration of Au NPs.	78
Figure 4.8:	(a) A graph of $\ln \alpha$ versus photon energy; (b) illustration of calculating Urbach energy of TZNE0.5 sample as an example after drawing a straight line from the linear part the graph of the sample.	79
Figure 4.9:	A graph of Urbach energy versus concentration of Au NPs.	79
Figure 4.10:	TEM image of Au NPs in (a) TZNE0.5-Au 0.2; (b) TZNE0.5-Au 0.3; (c) TZNE0.5-Au 0.4.	81
Figure 4.11:	Distribution of aspect ratio fitted with lognormal distribution functions of Au NPs in (a) TZNE0.5-Au 0.2 (containing 90 NPs); (b) TZNE0.5-Au 0.3 (containing 37 NPs); (c) TZNE0.5-Au 0.4 (containing 60 NPs). The frequency of a histogram of each sample represents the number of Au NPs counted in TEM image of that sample.	82
Figure 4.12:	Size distribution fitted with lognormal distribution functions of Au NPs in (a) TZNE0.5-Au 0.2 (containing 90 NPs); (b) TZNE0.5-Au 0.3 (containing 37 NPs); (c) TZNE0.5-Au 0.4 (containing 60 NPs). The frequency of a histogram of each sample represents the number of Au NPs counted in TEM image of that sample.	85
Figure 4.13:	SEM image of TZNE0.5-Au 0.4 glass sample.	87
Figure 4.14:	EDX spectrum of TZNE0.5-Au 0.4 glass sample.	89
Figure 4.15:	Excitation spectra of TZNE0.5 glass sample with emission wavelength set to be 550 nm.	90
Figure 4.16:	Emission spectrum of glass samples in wavelength of: (a) 300-520 nm, and (b) 530-640 nm respectively under	91



excitation wavelength of 522 nm.

- Figure 4.17: (a) – (c) Graphs of photoluminescence enhancement factor versus concentration of the Au NPs. 96
- Figure 4.18: Energy level diagram showing transitions of  $\text{Er}^{3+}$  ion between energy levels, interaction between  $\text{Er}^{3+}$  ion and gold NPs (Au NPs). GSA: ground state absorption; ESA: excited state absorption; LFE: local field enhancement; ET: energy transfer between Au NPs and  $\text{Er}^{3+}$  ion; ETU: energy transfer upconversion; NR: non-radiative decay; R: radiative decay. 99
- Figure 4.19: ATR-FTIR spectra of glass samples. 101
- Figure 4.20: Raman spectra of glass samples. It also shows FWHM of TZNE0.5 as an example to indicate width of its Raman spectrum. 104
- Figure 4.21: Raman spectrum of TZNE0.5-Au 0.4 showing Raman bands after performing deconvolution with Gaussian peaks. 105
- Figure 4.22: A graph of FWHM of Raman spectrum of the glass sample against concentration of the Au NPs. 107

## LIST OF ABBREVIATIONS AND SYMBOLS

$\text{TeO}_2$	- Tellurium dioxide
$\text{Na}_2\text{O}$	- Sodium oxide
$\text{ZnO}$	- Zinc oxide
$\text{Er}_2\text{O}_3$	- Erbium (III) oxide
$\text{Au}$	- Gold element
$\text{Te}$	- Tellurium element
$\text{Zn}$	- Zinc element
$\text{Na}$	- Sodium element
$\text{Er}$	- Erbium
$\text{O}$	- Oxygen element
$\text{C}$	- Carbon element
SPR	- Surface plasmon resonance
XRD	- X-ray diffraction
$n$	- Order of diffraction based on Bragg's law of XRD
$d$	- Spacing between two successive lattice planes of a crystal based on Bragg's law of XRD
$\theta$	- Angle of incidence of X-ray based on Bragg's law of XRD
$\lambda$	- Wavelength of an electromagnetic wave (for the case of spectroscopy) or an electron (for the case of de Broglie equation for operation of TEM) or a characteristic X-ray emitted by an atom (for the case of analysis of EDX)
$2\theta$	- Angle between an X-ray source and an X-ray detector
$\beta$	- Full-width at half-maximum (FWHM) of XRD peak due to

crystallite based on Debye-Scherrer equation

$\text{\AA}$	- Angstrom
Cu	- Copper
$K\alpha$	- K alpha of X-ray emitted by copper atoms in copper anode in XRD of current study
$K\alpha_1$	- K alpha 1 (One of K alpha X-ray doublets emitted by copper atoms in copper anode in XRD of current study)
$K\alpha_2$	- K alpha 2 (One of K alpha X-ray doublets emitted by copper atoms in copper anode in XRD of current study)
nm	- Nanometer
UV-Vis	- Ultraviolet-visible obtained from ultraviolet-visible spectroscopy
$A$	- Absorbance of a glass sample
$T$	- Transmittance of a glass sample given by $T = I/I_0$
a.u.	- Arbitrary unit (a unit used by absorbance for UV-Vis spectra, intensity of excitation and emission spectra of photoluminescence spectroscopy, and intensity of Raman spectra)
$\alpha$	- Absorption coefficient
$d$	- Thickness of a glass sample
$I_0$	- Intensity of incident light on a glass sample
$I$	- Intensity of transmitted light through a glass sample
$dI$	- The differential of intensity of light to represent the change of intensity of light as the light passes through the glass sample
$dx$	- The differential of distance travelled by light inside the glass sample to represent the amount of distance travelled by the light inside the glass sample

$h$	- Planck's constant equal to $6.626 \times 10^{-34}$ J s where J s is pronounced as Joule second
$\Delta L$	- Change in orbital angular momentum $L$ during a transition between two energy levels
$\Delta S$	- Change in spin angular momentum $S$ during a transition between two energy levels
$\Delta J$	- Change in total angular momentum $J$ during a transition between two energy levels where $J = L + S$
eV	- Electron volt (a unit used to quantify optical band gaps of glass samples and Urbach energy for UV-Vis spectral analysis)
$\hbar$	- Planck's constant $h$ divided by $2\pi$
$c$	- Speed of light in vacuum equal to $3.0 \times 10^8$ m/s
$\omega$	- Angular frequency of light, $\omega = 2\pi f$ with $f$ representing frequency of light
$E_{opt}$	- Optical band gap
$n$	- Exponent of a factor $(\hbar\omega - E_{opt})$ that depends on type of optical transition based on Davis-Mott theory
$E_{dir}$	- Direct optical band gap
$E_{indir}$	- Indirect optical band gap
$E_U$	- Urbach energy
$B$	- Energy-independent constant in mathematical expression of Davis-Mott theory
$\text{cm}^{-1}$	- Per unit centimeter (a unit of energy for energy level diagram in section of photoluminescence spectroscopy; a unit of wavenumber for FTIR, and a unit of Raman shift for Raman spectroscopy)
ATR	- Attenuated total reflection

- FTIR - Fourier Transform Infrared spectroscopy
- $n_i$  - Refractive index of a first medium that an infrared light is incident on based on principle of ATR-FTIR
- $n_r$  - Refractive index of a second medium that an infrared light passes through based on principle of ATR-FTIR
- $\theta_i$  - Angle of incidence of an infrared light based on principle of ATR-FTIR
- $\theta_r$  - Angle of refraction of an infrared light based on principle of ATR-FTIR
- TEM - Transmission electron microscopy
- $p$  - Momentum of an electron based on de Broglie's equation in physical principle of TEM
- $U$  - Electrostatic potential difference (or accelerating voltage) to accelerate electrons emitted by electron guns of TEM
- $\mu$  - Location parameter of a lognormal distribution function
- $\sigma$  - Shape parameter of a lognormal distribution function
- SEM - Scanning electron microscopy
- EDX - Energy dispersive X-ray spectroscopy; an abbreviation with the same meaning as that of EDS
- $E_i$  - Energy of an initial state of an electron of a given atom based on physical principle of EDX
- $E_f$  - Energy of a final state that has lower energy than that of an initial state of an electron of a given atoms based on physical principle of EDX
- $E_0$  - Beam energy of an incident electron beam in SEM and EDX
- keV - Kilo electron volt (used in EDX spectrum in the current study)

## LIST OF APPENDICES

	Page
Appendix A: Analysis of XRD peak due to Au NPs shown by (a) XRD pattern of TZNE0.5-Au 0.2 glass sample with an oval-shaped mark showing presence of the Au NPs due to diffraction of X-ray by them; (b) a diagram about estimating FWHM of an XRD peak due to the Au NPs in that glass sample; (c) a magnified view of two points for estimating the FWHM of the XRD peak.	134
Appendix B: Estimation of size of the Au NPs in TZNE0.5-Au 0.2 glass sample in Appendix A based on Table 1 (a), (b) and (c).	135
<p>Table 1 (a) shows parameters of an XRD peak for estimating the FWHM of the XRD peak and the size of the Au NPs in TZNE0.5-Au 0.2 glass sample.</p> <p>Table 1 (b) indicates FWHM and position of the XRD peak and their respective uncertainties for TZNE0.5-Au 0.2 glass sample where average and standard deviation are calculated with Microsoft Excel.</p> <p>Table 1 (c) depicts calculation of estimated size of the Au NPs and its uncertainty for TZNE0.5-Au 0.2 glass sample by using Debye-Scherrer equation given by equation (1), and equation (2) respectively.</p>	
Appendix C: Analysis of XRD peak due to Au NPs shown by (a) XRD pattern of TZNE0.5-Au 0.4 glass sample with an oval-shaped mark showing presence of the Au NPs due to diffraction of X-ray by them; (b) a diagram about estimating FWHM of an XRD peak due to the Au NPs in that glass sample; (c) a magnified view of two points for estimating the FWHM of the XRD peak.	137
Appendix D: Estimation of size of the Au NPs in TZNE0.5-Au 0.4 glass sample in Appendix C based on Table 2 (a), (b) and (c).	138
<p>Table 2 (a) shows parameters of an XRD peak for estimating the FWHM of the XRD peak and the size of the Au NPs in TZNE0.5-Au 0.4 glass sample.</p>	

Table 2 (b) indicates FWHM and position of the XRD peak and their respective uncertainties for TZNE0.5-Au 0.4 glass sample where average and standard deviation are calculated with Microsoft Excel.

Table 2 (c) depicts calculation of estimated size of the Au NPs and its uncertainty for TZNE0.5-Au 0.4 glass sample by using Debye-Scherrer equation given by equation (1), and equation (2) respectively.

- Appendix E: Result of nonlinear curve fit applied to a graph of direct optical band against concentration of the gold nanoparticles (Au NPs). Table 3 depicts equation of fitting function to fit the experimental data in Figure 4.6 and its parameters where  $y$  represents direct optical band gap  $E_{dir}$  while  $x$  represents concentration of the Au NPs in the unit of mol%. 140
- Appendix F: Result of nonlinear curve fit applied to a graph of indirect optical band against concentration of the gold nanoparticles (Au NPs). Table 4 depicts equation of fitting function to fit the experimental data in Figure 4.7 and its parameters where  $y$  represents direct optical band gap  $E_{indir}$  while  $x$  represents concentration of the Au NPs in the unit of mol%. 142
- Appendix G: Result of nonlinear curve fit applied to a graph of Urbach energy against concentration of the gold nanoparticles (Au NPs). Table 5 depicts equation of fitting function to fit the experimental data in Figure 4.9 and its parameters where  $y$  represents Urbach energy  $E_U$  while  $x$  represents concentration of the Au NPs in the unit of mol%. 144
- Appendix H: Results of testing for normality using level of significance equal to 0.05 for aspect ratio distribution of Au NPs in: (a) TZNE0.5-Au 0.2; (b) TZNE0.5-Au 0.3; (c) TZNE0.5-Au 0.4. 146
- Appendix I: Probability plot for aspect ratio distribution of Au NPs in: (a) TZNE0.5-Au 0.2; (b) TZNE0.5-Au 0.3; (c) TZNE0.5-Au 0.4 where the red solid lines (reference lines) in these figures are the normal distribution functions for each sample. 147
- Appendix J: Probability plot for aspect ratio distribution of Au NPs in: (a) TZNE0.5-Au 0.2; (b) TZNE0.5-Au 0.3; (c) TZNE0.5-Au 0.4 where the red solid lines (reference lines) are lognormal 148

distribution functions for each sample.

- Appendix K: Probability plots constructed with Origin Pro 2017 software to check whether the aspect ratio distribution of Au NPs (represented by the blue hollow circles) in: (a) TZNE0.5-Au 0.2; (b) TZNE0.5-Au 0.3; (c) TZNE0.5-Au 0.4 is parallel to green solid lines (reference lines) which are normal, lognormal, exponential, Gamma and Weibull distribution functions. 149
- Appendix L: Probability plots constructed with Origin Pro 9.0 software while using Hazen score method to check whether size distribution of Au NPs in: (a) TZNE0.5-Au 0.2; (b) TZNE0.5-Au 0.3; (c) TZNE0.5-Au 0.4 is parallel to the red solid lines (reference lines) in these figures which are the normal distribution functions for each sample. 152
- Appendix M: Probability plots constructed with Origin Pro 9.0 software while using Hazen score method to check whether size distribution of Au NPs in: (a) TZNE0.5-Au 0.2; (b) TZNE0.5-Au 0.3; (c) TZNE0.5-Au 0.4 is parallel to the red solid lines (reference lines) in these figures which are the lognormal distribution functions for each sample. 153
- Appendix N: Probability plots constructed with Origin Pro 2017 software to further check whether size distribution of Au NPs in: (a) TZNE0.5-Au 0.2; (b) TZNE0.5-Au 0.3; (c) TZNE0.5-Au 0.4 is parallel to the green solid lines (reference lines) which are normal, lognormal, exponential, Gamma and Weibull distribution functions. 154
- Appendix O: Characteristic X-rays of each element in TZNE0.5-Au 0.4 glass sample that are observed in the EDX spectrum, and their corresponding peak positions on X-ray energy scale of the EDX spectrum, transitions between electron shells of each element, and references. 157
- Appendix P: Relationship between photoluminescence enhancement factor and mean aspect ratio of Au NPs. 161
- Appendix Q: Three graphs of photoluminescence enhancement factor versus mean aspect ratio of Au NPs for each emission wavelength under excitation wavelength of 522 nm. They are labelled by (a), (b) and (c). 162



## REFERENCES

- Agilent Technologies, Inc. 2011a. *Agilent Technologies Cary 60 UV-Vis spectrophotometer: Guaranteed Specifications*. Santa Clara, CA: Agilent Technologies. Retrieved from [https://www.agilent.com/cs/library/specifications/public/5990-7881EN\\_Cary60\\_Specifications.pdf](https://www.agilent.com/cs/library/specifications/public/5990-7881EN_Cary60_Specifications.pdf) on 20 April 2019.
- Agilent Technologies, Inc. 2011b. *Agilent Technologies Cary 60 UV-Vis Spectrophotometer Brochure*. Santa Clara, CA: Agilent Technologies. Retrieved from [https://www.agilent.com/cs/library/brochures/5990-7789EN\\_Cary\\_60\\_UV-Vis\\_Brochure.pdf](https://www.agilent.com/cs/library/brochures/5990-7789EN_Cary_60_UV-Vis_Brochure.pdf) on 20 April 2019.
- Agilent Technologies, Inc. 2011c. *Agilent Technologies Cary 60 UV-Vis Spectrophotometer: Measuring Baseline-corrected Spectra on a Cary 60 UV-Vis*. Santa Clara, CA: Agilent Technologies. Retrieved from <https://www.agilent.com/cs/library/technicaloverviews/public/5990-7947EN.pdf> on 20 April 2019.
- Agilent Technologies, Inc. 2011d. *Agilent Technologies Cary Eclipse Fluorescence Spectrophotometer: Guaranteed Specifications*. Santa Clara, CA: Agilent Technologies.
- Agilent Technologies, Inc. 2011e. *Agilent Technologies Cary Eclipse Fluorescence Spectrophotometer: User's Guide*. Santa Clara, CA: Agilent Technologies. Retrieved from <https://www.agilent.com/cs/library/usermanuals/public/1758.pdf> on 20 April 2019.
- Agilent Technologies, Inc. 2011f. *Agilent Technologies Cary Eclipse Fluorescence Spectrophotometer Brochure*. Santa Clara, CA: Agilent Technologies. Retrieved from [https://www.agilent.com/cs/library/brochures/5990-7788EN\\_Cary\\_Eclipse\\_Brochure.pdf](https://www.agilent.com/cs/library/brochures/5990-7788EN_Cary_Eclipse_Brochure.pdf) on 20 April 2019.
- Ahmadi, F., Hussin, R. & Ghoshal, S.K. 2017. Spectroscopic Attributes of Sm<sup>3+</sup> Doped Magnesium Zinc Sulphophosphate Glass: Effect of Silver Nanoparticles Inclusion. *Optical Materials*, 73, 268-276.
- Akbari, B., Tavandashti, M. P. & Zandrahimi, M. 2011. Particle Size Characterization of Nanoparticles – A Practical Approach. *Iranian Journal of Materials Science & Engineering*, 8(2), 48-56.
- Akbarian, F., Dunn, B. S. & Zink, J. I. 1996. Porous Sol-gel Silicates Containing Gold Particles as Matrices for Surface-enhanced Raman Spectroscopy. *Journal of Raman spectroscopy*, 27(10), 775-783.



- Annappoorani, K., Murthy, N. S., Ravindran, T.R. & Marimuthu, K. 2016. Influence of  $\text{Er}^{3+}$  ion Concentration on Spectroscopic Properties and Luminescence Behavior in  $\text{Er}^{3+}$  Doped Strontium Telluroborate Glasses. *Journal of Luminescence*, 171, 19-26.
- Arcidiacono, S., Bieri, N. R., Poulikakos, D. & Grigoropoulos, C. P. 2004. On the Coalescence of Gold Nanoparticles. *International Journal of Multiphase Flow*, 30(7-8), 979-994.
- ASEQ Instruments. no yr. *Rm1 – Raman spectrometer*. Vancouver, Canada: ASEQ Instruments. Retrieved from [http://www.aseq-instruments.com/ASEQ\\_Raman.htm](http://www.aseq-instruments.com/ASEQ_Raman.htm) on 6 June 2018.
- Awang, A., Ghoshal, S.K., Sahar, M.R., Dousti, M.R., Amjad, R. J. & Nawaz, F. 2013. Enhanced Spectroscopic Properties and Judd-Ofelt Parameters of Er-doped Tellurite Glass: Effect of Gold Nanoparticles. *Current Applied Physics*, 13(8), 1813-1818.
- Awang, A., Ghoshal, S.K., Sahar, M.R., Dousti, M. R. & Nawaz, F. 2014. Growth of Au Nanoparticles Stimulate Spectroscopic Properties of  $\text{Er}^{3+}$ -doped  $\text{TeO}_2$ - $\text{ZnO}$ - $\text{Na}_2\text{O}$  Glasses. *Advanced Materials Research*, 895, 254-259.
- Awang, A., Ghoshal, S.K., Sahar, M.R. & Arifin, R. 2016. Tailoring Spectroscopic Properties of  $\text{Er}^{3+}$  Doped Zinc Sodium Tellurite Glass via Gold Nanoparticles. *Jurnal Teknologi*, 78(3-2), 139-144.
- Ayuni, J. N., Halimah, M. K., Talib, Z. A., Sidek, H. A. A., Daud, W. M., Zaidan, A. W. & Khamirul, A. M. 2011. Optical Properties of Ternary  $\text{TeO}_2$ - $\text{B}_2\text{O}_3$ - $\text{ZnO}$  Glass System. *IOP Conference Series: Materials Science and Engineering*, 17(1), 012027.
- Babu, S. S., Jang, K., Cho, E. J., Lee, H. & Jayasankar, C. K. 2007. Thermal, Structural and Optical Properties of  $\text{Eu}^{3+}$ -doped Zinc-tellurite Glasses. *Journal of Physics D: Applied Physics*, 40(18), 5767-5774.
- Baia, L., Baia, M., Kiefer, W., Popp, J. & Simon, S. 2006. Structural and Morphological Properties of Silver Nanoparticles-phosphate Glass Composites. *Chemical Physics*, 327(1), 63-69.
- Baia, L. & Simon, S. 2007. UV-Vis and TEM Assessment of Morphological Features of Silver Nanoparticles from Phosphate Glass Matrices. In A. Méndez-Vilas & J. Díaz (eds.), *Modern Research and Educational Topics in Microscopy*, pp. 576-583. Badajoz, Spain: Formatex. Retrieved from <http://citeseerx.ist.psu.edu/viewdoc/download?doi=10.1.1.605.2338&rep=rep1&type=pdf> on 15 August 2018.
- Ballarin, B., Cassani, M. C., Tonelli, D., Boanini, E., Albonetti, S., Blosi, M. & Gazzano, M. 2010. Gold Nanoparticles-containing Membranes from In Situ

- Reduction of a Gold(III)-aminoethylimidazolium Aurate Salt. *The Journal of Physical Chemistry C*, 114(21), 9693-9701.
- Bearden, J. A. 1967. X-ray Wavelengths. *Reviews of Modern Physics*, 39(1), 78-124.
- Bhattacharya, S. & Ghosh, A. 2010. Relaxation Dynamics in Superionic Molybdate Glass Nanocomposites Embedded with  $\alpha$ -AgI Nanoparticles. *The Journal of Physical Chemistry C*, 114(13), 5745-5750.
- Bowen, P. 2007. Particle Size Distribution Measurement from Millimetres to Nanometers and from Rods to Platelets. *Journal of Dispersion Science and Technology*, 23(5), 631-662.
- Brance, U. R., Drummond, I. W., Finbow, D., Harden, E. H. & Kenway, P. 1978. 27. Hydrocarbon Contamination in Vacuum Dependent Scientific Instruments. *Vacuum*, 28(10-11) 489-496.
- Carnall, W. T., Fields, P. R. & Rajnak, K. 1968. Electronic Energy Levels in the Trivalent Lanthanide Aquo Ions. I.  $\text{Pr}^{3+}$ ,  $\text{Nd}^{3+}$ ,  $\text{Pm}^{3+}$ ,  $\text{Sm}^{3+}$ ,  $\text{Dy}^{3+}$ ,  $\text{Ho}^{3+}$ ,  $\text{Er}^{3+}$ , and  $\text{Tm}^{3+}$ . *The Journal of Chemical Physics*, 49(10), 4424-4442.
- Çelikbilek, M., Ersundu, A.E., Solak, N. & Aydin, S. 2011. Crystallization Kinetics of the Tungsten-tellurite Glasses. *Journal of Non-Crystalline Solids*, 357(1), 88-95.
- Cherif, A., Kanoun, A. & Maaref, H. 2011. Up-conversion Fluorescence Dynamics in  $\text{Er}^{3+}/\text{Yb}^{3+}$  Co-doped Tellurite Glasses. *Optica Applicata*, 41(1), 235-245. Retrieved from <https://www.semanticscholar.org/paper/Up-conversion-fluorescence-dynamics-in-Er3-Yb3-co-Cherif-Kanoun/76df1e9baef857215a403b0ff95fdd3bce4797db> on 20 April 2017.
- Constantin, D. 2015. Why the Aspect Ratio? Shape Equivalence for the Extinction Spectra of Gold Nanoparticles. *The European Physical Journal E*, 38(11), 116.
- de Araújo, C. B. & Kassab, L. R. P. 2017. Linear and Non-linear Optical Properties of Some Tellurium Oxide Glasses. In V.A.G. Rivera & D. Manzani (eds.). *Technological Advances in Tellurite Glasses: Properties, Processing, and Applications*, pp. 15-37. Cham, Switzerland: Springer.
- Dellith, J. & Wendt, M. 2007. The M Emission Spectrum of  $^{68}\text{Er}$ mium. *Microscopy and Microanalysis*, 13(3), 191-195.
- Dellith, J. & Wendt, M. 2008. The M Emission Spectra of the Heavy Rare Earth Elements  $67 \leq Z \leq 71$ . *Microchimica Acta*, 161(3-4), 475-478.

- Deslattes, R. D., Kessler, Jr., E. G., Indelicato, P., de Billy, L., Lindroth, E. & Anton, J. 2003. X-ray Transition Energies: New Approach to a Comprehensive Evaluation. *Reviews of Modern Physics*, 75(1), 35-99.
- Devi, A. R. & Jayasankar, C.K. 1996. Optical Properties of Er<sup>3+</sup> Ions in Lithium Borate Glasses and Comparative Energy Level Analyses of Er<sup>3+</sup> Ions in Various Glasses. *Journal of Non-Crystalline Solids*, 197(2-3), 111-128.
- Dieke, G. H. & Crosswhite, H. M. 1963. The Spectra of the Doubly and Triply Ionized Rare Earths. *Applied Optics*, 2(7), 675-686.
- Dousti, M.R. 2013. Efficient Infrared-to-visible Upconversion Emission in Nd<sup>3+</sup>-doped PbO-TeO<sub>2</sub> Glass Containing Silver Nanoparticles. *Journal of Applied Physics*, 114(11), 113105. Retrieved from [https://www.researchgate.net/profile/M\\_Reza\\_Dousti/publication/257536342\\_Efficient\\_infrared-to-visible\\_upconversion\\_emission\\_in\\_Nd3-doped\\_PbO-TeO2\\_glass\\_containing\\_silver\\_NPs/links/553a45880cf245bdd762e1cb.pdf](https://www.researchgate.net/profile/M_Reza_Dousti/publication/257536342_Efficient_infrared-to-visible_upconversion_emission_in_Nd3-doped_PbO-TeO2_glass_containing_silver_NPs/links/553a45880cf245bdd762e1cb.pdf) on 20 May 2018.
- Dousti, M. R., Sahar, M.R., Amjad, R.J., Ghoshal, S.K. & Awang, A. 2013a. Surface Enhanced Raman Scattering and Up-conversion Emission by Silver Nanoparticles in Erbium-zinc-tellurite Glass. *Journal of Luminescence*, 143, 368-373.
- Dousti, M. R., Sahar, M.R., Ghoshal, S.K., Amjad, R.J. & Samavati, A.R. 2013b. Effect of AgCl on Spectroscopic Properties of Erbium Doped Zinc Tellurite Glass. *Journal of Molecular Structure*, 1035, 6-12.
- Dousti, M. R. & Hosseinian, S.R. 2014. Enhanced Upconversion Emission of Dy<sup>3+</sup>-doped Tellurite Glass by Heat-treated Silver Nanoparticles. *Journal of Luminescence*, 154, 218-223.
- Dousti, M. R., Amjad, R. J. & Mahraz, Z. A. S. 2015a. Enhanced Green and Red Upconversion Emissions in Er<sup>3+</sup>-doped Boro-tellurite Glass Containing Gold Nanoparticles. *Journal of Molecular Structure*, 1079, 347-352.
- Dousti, M.R., Amjad, R.J., Sahar, M.R., Zabidi, Z.M., Alias, A.N. & de Camargo, A.S.S. 2015b. Er<sup>3+</sup>-doped Zinc Tellurite Glasses Revisited: Concentration Dependent Chemical Durability, Thermal Stability and Spectroscopic Properties. *Journal of Non-Crystalline Solids*, 429, 70-78.
- Dousti, M.R. & Amjad, R.J. 2016a. Plasmon Assisted Luminescence in Rare Earth Doped Glasses. In C. D. Geddes (ed.). *Reviews in Plasmonics 2015*, pp. 340. Cham, Switzerland: Springer.
- Dousti, M.R. & Amjad, R.J. 2016b. Plasmon Assisted Luminescence in Rare Earth Doped Glasses. In C. D. Geddes (ed.). *Reviews in Plasmonics 2015*, pp. 358. Cham, Switzerland: Springer.

- Dousti, M.R. & Amjad, R.J. 2016c. Plasmon Assisted Luminescence in Rare Earth Doped Glasses. In C. D. Geddes (ed.). *Reviews in Plasmonics 2015*, pp. 339-345. Cham, Switzerland: Springer.
- Dravid, V. 2016, December. *NUANCE Atomic and Nanoscale Characterization Experimental Center*. Poster session presented at the meeting of the National Science Foundation, Arlington, VA. Retrieved from <http://www.nseresearch.org/2016/posters/NUANCE-Poster-2016.pdf> on 20 June 2018.
- Echlin, P. 2009. Sample Surface Charge Elimination. In *Handbook of Sample Preparation for Scanning Electron Microscopy and X-ray Microanalysis*, pp. 247-298. New York, NY: Springer.
- Egerton, R.F. 2005a. The Transmission Electron Microscope. In *Physical Principles of Electron Microscopy: An Introduction to TEM, SEM, and AEM*, pp. 57-86. New York, NY: Springer.
- Egerton, R.F. 2005b. The Scanning Electron Microscope. In *Physical Principles of Electron Microscopy: An Introduction to TEM, SEM, and AEM*, pp. 125-126. New York, NY: Springer.
- Egerton, R.F. 2005c. The Scanning Electron Microscope. In *Physical Principles of Electron Microscopy: An Introduction to TEM, SEM, and AEM*, pp. 137. New York, NY: Springer.
- Egerton, R. F. 2005d. Analytical Electron Microscopy. In *Physical Principles of Electron Microscopy: An Introduction to TEM, SEM, and AEM*, pp. 160. New York, NY: Springer.
- El-Deen, L.M. S., Al Salhi, M.S. & Elkholy, M. M. 2008. IR and UV Spectral Studies for Rare Earth Doped Tellurite Glasses. *Journal of Alloys and Compounds*, 465(1-2), 333-339.
- El-Mallawany, R. 2002a. Infrared and Raman Spectra of Tellurite Glasses. In *Tellurite Glass Handbook, Physical Properties and Data 1<sup>st</sup> Edition*, pp. 488-520. Boca Raton, Florida: CRC Press.
- El-Mallawany, R. 2002b. Introduction to Tellurite Glasses. In *Tellurite Glasses: Physical Properties and Data 1<sup>st</sup> Edition*, pp. 17-39. Boca Raton, FL: CRC Press.
- El-Mallawany, R. 2002c. Thermal Properties of Tellurite Glasses. In *Tellurite Glass Handbook, Physical Properties and Data 1<sup>st</sup> Edition*, pp. 204-205. Boca Raton, FL: CRC Press.
- El-Mallawany, R. 2002d. Optical Properties of Tellurite Glasses in the Ultraviolet Region. In *Tellurite Glass Handbook, Physical Properties and Data 1<sup>st</sup> Edition*, pp. 436-442. Boca Raton, FL: CRC Press.

- El-Mallawany, R. 2002e. Infrared and Raman spectra of Tellurite Glasses. *In Tellurite Glass Handbook, Physical Properties and Data 1<sup>st</sup> Edition*, pp. 481. Boca Raton, Florida: CRC Press.
- El-Mallawany, R. 2002f. Infrared and Raman spectra of Tellurite Glasses. *In Tellurite Glass Handbook, Physical Properties and Data 1<sup>st</sup> Edition*, pp. 506-520. Boca Raton, Florida: CRC Press.
- El-Mallawany, R., Dirar Abdalla, M. & Abbas Ahmed, I. 2008. New Tellurite Glass: Optical Properties. *Materials Chemistry and Physics*, 109(2-3), 291-296.
- Ennos, A. E. 1953. The Origin of Specimen Contamination in the Electron Microscope. *British Journal of Applied Physics*, 4(4), 101-106.
- Eraiah, B. 2017. Optical Properties of Silver-vanadium-phosphate Glasses. *Mapana Journal of Sciences*, 16(1), 1-7.
- Erol, M., Küçükbayrak, S. & Ersoy-Meriçboyu, A. 2008. Comparison of the Properties of Glass, Glass-ceramic and Ceramic Materials Produced from Coal Fly Ash. *Journal of Hazardous Materials*, 153(1-2), 418-425.
- Eustis, S. & El-Sayed, M. A. 2006. Why Gold Nanoparticles Are More Precious than Pretty Gold: Noble Metal Surface Plasmon Resonance and Its Enhancement of the Radiative and Nonradiative Properties of Nanocrystals of Different Shapes. *Chemical Society Reviews*, 35(3), 209-217.
- Farahmandjou, M. & Salehizadeh, S. A. 2013. The Optical Band Gap and the Tailing States Determination in Glasses of TeO<sub>2</sub>-V<sub>2</sub>O<sub>5</sub>-K<sub>2</sub>O System. *Glass Physics and Chemistry*, 39(5), 473-479.
- Fatimah, S., Sahar, M. R., Ghoshal, S. K., Ariffin, R. & Hamzah, K. 2014. Optical Absorption of Erbium Doped Tellurite Glass. *Advanced Materials Research*, 895, 245-249.
- Faznny, M. F., Halimah, M. K. & Azlan, M. N. 2016. Effect of Lanthanum Oxide on Optical Properties of Zinc Borotellurite Glass System. *Journal of Optoelectronics and Biomedical Materials*, 8(2), 49-59.
- Ferrell, S. K. 2015. *Effects of Metal and Semiconducting Nanoparticles on the Fluorescence and Optical Band Gap of Dy<sup>3+</sup> Doped Lead Borate and Bismuth Borate Glasses*. (Master's Thesis) Western Illinois University. Retrieved from [https://www.researchgate.net/publication/282735230\\_EFFECTS\\_OF\\_METAL\\_AND\\_SEMICONDUCTING\\_NPS\\_ON\\_THE\\_FLUORESCENCE\\_AND\\_OPTICAL\\_BAND\\_GAP\\_OF\\_Dy3\\_DOPED\\_LEAD\\_BORATE\\_AND\\_BISMUTH\\_BORATE\\_GLASSES?enrichId=rgreq-c29c92d6c100cbf29b037887116f7b61-XXX&enrichSource=Y292ZXJQYWdlOzI4MjcZNTIzMDtBUzozMzAxODYxOTAwMTY1MTNAMTQ1NTczMzkzMDM1MQ%3D%3D&el=1\\_x\\_2&\\_esc=publication](https://www.researchgate.net/publication/282735230_EFFECTS_OF_METAL_AND_SEMICONDUCTING_NPS_ON_THE_FLUORESCENCE_AND_OPTICAL_BAND_GAP_OF_Dy3_DOPED_LEAD_BORATE_AND_BISMUTH_BORATE_GLASSES?enrichId=rgreq-c29c92d6c100cbf29b037887116f7b61-XXX&enrichSource=Y292ZXJQYWdlOzI4MjcZNTIzMDtBUzozMzAxODYxOTAwMTY1MTNAMTQ1NTczMzkzMDM1MQ%3D%3D&el=1_x_2&_esc=publication) CoverPdf on 15 July 2018.
- Florez, A., Messaddeq, Y., Malta, O.L. & Aegerter, M.A. 1995. Optical Transition Probabilities and Compositional Dependence of Judd-Ofelt Parameters of

- Er<sup>3+</sup> Ions in Fluoroindate Glass. *Journal of Alloys and Compounds*, 227(2), 135-140.
- Fultz, B. & Howe, J. M. 2013. Diffraction and X-ray Powder Diffractometer. In *Transmission Electron Microscopy and Diffractometry of Materials 4<sup>th</sup> Edition*, pp. 1-52. Berlin, Heidelberg: Springer.
- Garcia, M.A. 2011. Surface Plasmons in Metal Nanoparticles: Fundamentals and Applications. *Journal of Physics D: Applied Physics*, 44(28), 283001.
- Ghoshal, S.K., Awang, A., Sahar, M.R., Amjad, R.J. & Dousti, M.R. 2013. Spectroscopic and Structural Properties of TeO<sub>2</sub>-ZnO-Na<sub>2</sub>O-Er<sub>2</sub>O<sub>3</sub>-Au Glasses. *Chalcogenide Glasses*, 10(10), 411-420.
- Ghoshal, S.K., Awang, A., Sahar, M.R. & Arifin, R. 2015. Gold Nanoparticles Assisted Surface Enhanced Raman Scattering and Luminescence of Er<sup>3+</sup> Doped Zinc-sodium Tellurite Glass. *Journal of Luminescence*, 159, 265-273.
- Goldstein, J., Newbury, D. E., Echlin, P., Joy, D. C., Romig, Jr., A. D., Lyman, C. E., Fiori, C. & Lifshin, E. 1992. Qualitative X-ray Analysis. In *Scanning Electron Microscopy and X-ray Microanalysis: A Text for Biologists, Materials Scientists, and Geologists 2<sup>nd</sup> Edition*, pp. 349-352. New York, NY: Plenum Press.
- Goldstein, J. I., Newbury, D. E., Echlin, P., Joy, D. C., Lyman, C. E., Lifshin, E., Sawyer, L. & Michael, J. R. 2003a. Electron Beam-specimen Interactions. In *Scanning Electron Microscopy and X-ray Microanalysis 3<sup>rd</sup> Edition*, pp. 61-98. New York, NY: Kluwer Academic/Plenum Publishers.
- Goldstein, J. I., Newbury, D. E., Echlin, P., Joy, D. C., Lyman, C. E., Lifshin, E., Sawyer, L. & Michael, J. R. 2003a. Electron Beam-specimen Interactions. In *Scanning Electron Microscopy and X-ray Microanalysis 3<sup>rd</sup> Edition*, pp. 75-98. New York, NY: Kluwer Academic/Plenum Publishers.
- Goldstein, J. I., Newbury, D. E., Echlin, P., Joy, D. C., Lyman, C. E., Lifshin, E., Sawyer, L. & Michael, J. R. 2003b. Image Formation and Interpretation. In *Scanning Electron Microscopy and X-ray Microanalysis 3<sup>rd</sup> Edition*, pp. 99-103. New York, NY: Kluwer Academic/Plenum Publishers.
- Goldstein, J. I., Newbury, D., Echlin, P., Joy, D. C., Lyman, C. E., Lifshin, E., Sawyer, L. & Michael, J. R. 2003c. Generation of X-rays in the SEM Specimen. In *Scanning Electron Microscopy and X-ray Microanalysis 3<sup>rd</sup> Edition*, pp. 274-281. New York, NY: Kluwer Academic/Plenum Publishers.
- Goldstein, J. I., Newbury, D. E., Michael, J. R., Ritchie, N. W.M., Scott, J. H. J. & Joy, D. C. 2018a. Image Formation. In *Scanning Electron Microscopy and X-ray Microanalysis 4<sup>th</sup> Edition*, pp. 94. New York, NY: Springer.

- Goldstein, J. I., Newbury, D. E., Michael, J. R., Ritchie, N. W.M., Scott, J. H. J. & Joy, D. C. 2018b. Energy Dispersive X-ray Spectrometry: Physical Principles and User-selected Parameters. *In Scanning Electron Microscopy and X-ray Microanalysis 4<sup>th</sup> Edition*, pp. 210-212. New York, NY: Springer.
- Goldstein, J. I., Newbury, D. E., Michael, J. R., Ritchie, N. W.M., Scott, J. H. J. & Joy, D. C. 2018c. Image Defects. *In Scanning Electron Microscopy and X-ray Microscopy 4<sup>th</sup> Edition*, pp. 143. New York, NY: Springer.
- Goldstein, J. I., Newbury, D. E., Michael, J. R., Ritchie, N. W.M., Scott, J. H. J. & Joy, D. C. 2018d. Energy Dispersive X-ray Spectrometry: Physical Principles and User-selected Parameters. *In Scanning Electron Microscopy and X-ray Microscopy 4<sup>th</sup> Edition*, pp. 213. New York, NY: Springer.
- Goldstein, J. I., Newbury, D. E., Michael, J. R., Ritchie, N. W.M., Scott, J. H. J. & Joy, D. C. 2018e. Qualitative Elemental Analysis by Energy Dispersive X-ray Spectrometry. *In Scanning Electron Microscopy and X-ray Microscopy 4<sup>th</sup> Edition.*, pp. 266-272. New York, NY: Springer.
- Goldstein, J. I., Newbury, D. E., Michael, J. R., Ritchie, N. W.M., Scott, J. H. J. & Joy, D. C. 2018f. Qualitative Elemental Analysis by Energy Dispersive X-ray Spectrometry. *In Scanning Electron Microscopy and X-ray Microscopy 4<sup>th</sup> Edition*, pp. 275-278. New York, NY: Springer.
- Goldstein, J. I., Newbury, D. E., Michael, J. R., Ritchie, N. W.M., Scott, J. H. J. & Joy, D. C. 2018g. Qualitative Elemental Analysis by Energy Dispersive X-ray Spectrometry. *In Scanning Electron Microscopy and X-ray Microscopy 4<sup>th</sup> Edition*, pp. 281. New York, NY: Springer.
- Goldstein, J. I., Newbury, D. E., Michael, J. R., Ritchie, N. W.M., Scott, J. H. J. & Joy, D. C. 2018h. X-rays. *In Scanning Electron Microscopy and X-ray Microscopy 4<sup>th</sup> Edition*, pp. 42-44. New York, NY: Springer.
- Goodhew, P. J., Humphreys, J. & Beanland, R. 2001a. The Scanning Electron Microscope. *In Electron Microscopy and Analysis 3<sup>rd</sup> Edition*, pp. 122-131. London and New York: Taylor & Francis.
- Goodhew, P. J., Humphreys, J. & Beanland, R. 2001b. Chemical Analysis in the Electron Microscope. *In Electron Microscopy and Analysis 3<sup>rd</sup> Edition*, pp. 169-173. London and New York: Taylor & Francis.
- Goodhew, P. J., Humphreys, J. & Beanland, R. 2001c. Chemical Analysis in the Electron Microscope. *In Electron Microscopy and Analysis 3<sup>rd</sup> Edition*, pp. 180. London and New York: Taylor & Francis.
- Gryczynski, Z., Matveeva, E. G., Calander, N., Zhang, J., Lakowicz, J. R., Gryczynski, I. 2007. Surface Plasmon Coupled Emission. *In* M. L.



- Brongersma & P. G. Kik (eds.). *Surface Plasmon Nanophotonics*, pp. 247-248. Dordrecht, The Netherlands: Springer.
- Halimah, M.K., Daud, W.M., Sidek, H.A.A., Zaidan, A.W. & Zainal, A.S. 2010. Optical Properties of Ternary Tellurite Glasses. *Materials Science-Poland*, 28(1), 173-180.
- Han, M., Oh, S.J., Park, J. H. & Park, H. L. 1993. X-ray Photoelectron Spectroscopy Study of CaS:Eu and SrS:Eu Phosphors. *Journal of Applied Physics*. 73(9), 4546-4549.
- Holton, I. 2012, May. Is Energy-dispersive Spectroscopy in the SEM a Substitute for Electron Probe Microanalysis? *Microscopy and Analysis*, 26(4): S4-S7 (AM). Retrieved from <https://microscopy-analysis.com/magazine/issues/energy-dispersive-spectroscopy-sem-substitute-electron-probe-microanalysis> on 20 June 2018.
- Hu, Y., Qiu, J., Song, Z. & Zhou, D. 2014. Ag<sub>2</sub>O Dependent Up-conversion Luminescence Properties in Tm<sup>3+</sup>/Er<sup>3+</sup>/Yb<sup>3+</sup> Co-doped Oxyfluorogermanate Glasses. *Journal of Applied Physics*, 115(8), 083512-1 - 6.
- Huang, Y.D., Mortier, M. & Auzel, F. 2001a. Stark Levels Analysis for Er<sup>3+</sup>-doped Oxide Glasses: Germanate and Silicate. *Optical Materials*, 15(4), 243-260.
- Huang, Y.D., Mortier, M. & Auzel, F. 2001b. Stark Level Analysis for Er<sup>3+</sup>-doped ZBLAN Glass. *Optical Materials*, 17(4), 501-511.
- Jaba, N., Mermet, A., Duval, E. & Champagnon, B. 2005. Raman Spectroscopy of Er<sup>3+</sup>-doped Zinc Tellurite Glasses. *Journal of Non-Crystalline Solids*, 351(10-11), 833-837.
- Jain, P. K., Huang, X., El-Sayed, I. H. & El-Sayed, M. A. 2007. Review of Some Interesting Surface Plasmon Resonance-enhanced Properties of Noble Metal Nanoparticles and Their Applications to Biosystems. *Plasmonics*, 2(3), 107-118.
- Jha, A., Shen, S. & Naftaly, M. 2000. Structural Origin of Spectral Broadening of 1.5- $\mu$ m Emission in Er<sup>3+</sup>-doped Tellurite Glasses. *Physical Review B*, 62(10), 6215-6227.
- Jlassi, I., Elhouichet, H. & Ferid, M. 2011. Thermal and Optical Properties of Tellurite Glasses Doped Erbium. *Journal of Materials Science*, 46(3), 806-812.
- Jørgensen, C. K. & Judd, B. R. 1964. Hypersensitive Pseudoquadrupole Transitions in Lanthanides. *Molecular Physics: An International Journal at the Interface between Chemistry and Physics*, 8(3), 281-290.
- Jose, R. & Ohishi, Y. 2007. Ultra-broadband Raman Gain Media for Photonics Device Applications. *Optical Components and Materials IV*, 6469, 64690K.
- Kamitsos, E.I. 2015. Infrared Spectroscopy of Glasses. In M. Affatigato (ed.). *Modern Glass Characterization*, pp. 77-78. Hoboken, NJ: John Wiley & Sons.

- Karmakar, B., Som, T., Singh, S. P. & Nath, M. 2010. Nanometal-glass Hybrid Nanocomposites: Synthesis, Properties and Applications. *Transactions of the Indian Ceramic Society*, 69(3), 171-186.
- Karmakar, B. 2016a. Fundamentals of Glass and Glass Nanocomposites. In B. Karmakar, K. Rademann & A. L. Stepanov (eds.). *Glass Nanocomposites: Synthesis, Properties and Applications 1<sup>st</sup> Edition*, pp. 6-12. Oxford, UK & Cambridge, USA: Elsevier.
- Karmakar, B. 2016b. Fundamentals of Glass and Glass Nanocomposites. In B. Karmakar, K. Rademann & A. L. Stepanov (eds.). *Glass Nanocomposites: Synthesis, Properties and Applications 1<sup>st</sup> Edition*, pp. 21-22. Oxford, UK & Cambridge, USA: Elsevier.
- Karmakar, B. 2016c. Fundamentals of Glass and Glass Nanocomposites. In B. Karmakar, K. Rademann & A. L. Stepanov (eds.). *Glass Nanocomposites: Synthesis, Properties and Applications 1<sup>st</sup> Edition*, pp. 29-34. Oxford, UK & Cambridge, USA: Elsevier.
- Karmakar, B. 2016d. Fundamentals of Glass and Glass Nanocomposites. In B. Karmakar, K. Rademann & A. L. Stepanov (eds.). *Glass Nanocomposites: Synthesis, Properties and Applications 1<sup>st</sup> Edition*, pp. 16-17. Oxford, UK & Cambridge, USA: Elsevier.
- Karmakar, B. 2016e. Fundamentals of Glass and Glass Nanocomposites. In B. Karmakar, K. Rademann & A. L. Stepanov (eds.). *Glass Nanocomposites: Synthesis, Properties and Applications 1<sup>st</sup> Edition*, pp. 38-41. Oxford, UK & Cambridge, USA: Elsevier.
- Kenyon, A.J. 2002. Recent Developments in Rare-earth Doped Materials for Optoelectronics. *Progress in Quantum Electronics*, 26(4-5), 225-284.
- Khondker, A. & Lakhani, S. 2015. X-Ray Diffraction: A Comprehensive Explanation for Multipurpose Research. *International Journal of Interdisciplinary Research and Innovations*, 3(1), 60-64. Retrieved from <http://www.researchpublish.com/journal/IJIRI/Issue-1-January-2015-March-2015/0> on 20 May 2018.
- Klinger, M.I. 2013. General Description of Glasses and Glass Transition. In *Glassy Disordered Systems: Glass Formation and Universal Anomalous Low-Energy Properties*, pp. 5-6. Toh Tuck Link, Singapore: World Scientific.
- Kortright, J. B. & Thompson, A. C. 2009. X-ray Properties of Elements: X-ray Emission Energies. In A. C. Thompson (ed.), *X-ray Data Booklet 3<sup>rd</sup> Edition*, 1-8 – 1-27.
- Krishnaiah, K. V., Marques-Hueso, J. & Kashyap, R. 2017. Broadband Emission in Tellurite Glasses. In V.A.G. Rivera & D. Manzani (eds.). *Technological*

*Advances in Tellurite Glasses: Properties, Processing, and Applications*, pp. 158-163. Cham, Switzerland: Springer.

- Krishnaiah, K. V., Venkataiah, G., Marques-Hueso, J., Dharmaiah, P., Jayasankar, C.K. & Richards, B.S. 2015. Broadband Near-infrared Luminescence and Visible Upconversion of Er<sup>3+</sup>-doped Tungstate-tellurite Glasses. *Science of Advanced Materials*, 7(2), 345-353.
- Kumar, K., Rai, S.B. & Rai, D.K. 2006. Upconversion Studies in Er<sup>3+</sup> Doped TeO<sub>2</sub>-M<sub>2</sub>O (M=Li, Na and K) Binary Glasses. *Solid State Communications*, 139(7), 363-369.
- Kumar, S. & Sood, A.K. 2016. Ultrafast Response of Plasmonic Nanostructures. In C. D. Geddes (ed.). *Reviews in Plasmonics 2015*, pp. 136. Cham, Switzerland: Springer.
- Lakowicz, J. R. 2006a. Instrumentation for Fluorescence Spectroscopy. In *Principles of Fluorescence Spectroscopy 3<sup>rd</sup> Edition*, pp. 27-28. New York, NY: Springer.
- Lakowicz, J. R. 2006b. Instrumentation for Fluorescence Spectroscopy. In *Principles of Fluorescence Spectroscopy 3<sup>rd</sup> Edition*, pp. 30-31. New York, NY: Springer.
- Lakshminarayana, G., Kaky, K.M., Baki, S.O., Ye, S., Lira, A., Kityk, I.V. & Mahdi, M.A. 2016. Concentration Dependent Structural, Thermal, and Optical Features of Pr<sup>3+</sup>-doped Multicomponent Tellurite Glasses. *Journal of Alloys and Compounds*, 686, 769-784.
- Lakshminarayana, G., Kaky, K.M., Baki, S.O., Lira, A., Nayar, P., Kityk, I.V. & Mahdi, M.A. 2017. Physical, Structural, Thermal, and Optical Spectroscopy Studies of TeO<sub>2</sub>-B<sub>2</sub>O<sub>3</sub>-MoO<sub>3</sub>-ZnO-R<sub>2</sub>O (R=Li, Na, and K)/MO (M = Mg, Ca, and Pb) Glasses. *Journal of Alloys and Compounds*, 690, 799-816.
- Lee, D. K., Park, S. I., Lee, J. K. & Hwang, N. M. 2007. A Theoretical Model for Digestive Ripening. *Acta Materialia*, 55(15), 5281-5288.
- Lee, D. K. & Hwang, N. M. 2009. Thermodynamics and Kinetics of Monodisperse Alloy Nanoparticles Synthesized through Digestive Ripening. *Scripta Materialia*, 61(3), 304-307.
- Lin, X. M., Sorensen, C. M. & Klabunde, K. J. 2000. Digestive Ripening, Nanophase Segregation and Superlattice Formation in Gold Nanocrystal Colloids. *Journal of Nanoparticle Research*, 2(2), 157-164.
- Lin, H., Zhang, Y.Y. & Pun, E.Y. 2008. Fluorescence Investigation of Ho<sup>3+</sup> in Yb<sup>3+</sup> Sensitized Mixed-alkali Bismuth Gallate Glass. *Spectrochimica Acta Part A: Molecular and Biomolecular Spectroscopy*, 71(4), 1547-1550.

- Long, D.A. 2002a. Survey of Light-scattering Phenomena. *In The Raman Effect: A Unified Treatment of the Theory of Raman Scattering by Molecules*, pp. 3-18. West Sussex, England: John Wiley and Sons.
- Long, D. A. 2002b. Classical Theory of Rayleigh and Raman Scattering. *In The Raman Effect: A Unified Treatment of the Theory of Raman Scattering by Molecules*, pp. 47-48. West Sussex, England: John Wiley and Sons.
- Lövestam, G., Rauscher, H., Roebben, G., Klüttgen, B. S., Gibson, N., Putaud, J. & Stamm, H. 2010. *Considerations on a Definition of Nanomaterial for Regulatory Purposes*. JRC Publication No. JRC58726. European Union: Joint Research Centre. Retrieved from <https://ec.europa.eu/jrc/en/publication/reference-reports/considerations-definition-nanomaterial-regulatory-purposes> on 20 August 2018.
- Maheshvaran, K., Veeran, P.K. & Marimuthu, K. 2013. Structural and Optical Studies on Eu<sup>3+</sup> Doped Boro Tellurite Glasses. *Solid State Sciences*, 17, 54-62.
- Malta, O.L., Santa-Cruz, P.A., De Sa, G.F. & Auzel, F. 1985. Fluorescence Enhancement Induced by the Presence of Small Silver Particles in Eu<sup>3+</sup> Doped Materials. *Journal of Luminescence*, 33(3), 261-272.
- Malta, O. L. & Carlos, L. D. 2003. Intensities of 4f-4f Transitions in Glass Materials. *Química Nova*, 26(6), 889-895.
- Marjanovic, S., Toulouse, J., Jain, H., Sandmann, C., Dierolf, V., Kortan, A.R., Kopylov, N. & Ahrens, R.G. 2003. Characterization of New Erbium-doped Tellurite Glasses and Fibers. *Journal of Non-Crystalline Solids*, 322(1-3), 311-318.
- McClure, D. S. & Kiss, Z. 1963. Survey of the Spectra of the Divalent Rare-earth Ions in Cubic Crystals. *Journal of Chemical Physics*, 39(12), 3251-3257.
- Mitra, A. & De, G. 2016. Sol-gel Synthesis of Metal Nanoparticle Incorporated Oxide Films on Glass. *In B. Karmakar, K. Rademann & A. L. Stepanov (eds.). Glass - Nanocomposites: Synthesis, Properties and Applications 1<sup>st</sup> Edition*, pp. 147. Oxford, UK & Cambridge, USA: Elsevier.
- Munoz-Martín, D., Villegas, M.A., Gonzalo, J. & Fernández-Navarro, J.M. 2009. Characterisation of Glasses in the TeO<sub>2</sub>-WO<sub>3</sub>-PbO System. *Journal of the European Ceramic Society*, 29(14), 2903-2913.
- Murugan, G. S., Suzuki, T. & Ohishi, Y. 2006. Raman Characteristics and Nonlinear Optical Properties of Tellurite and Phosphotellurite Glasses Containing Heavy Metal Oxides with Ultrabroad Raman Bands. *Journal of Applied Physics Letters*, 100(2), 023107.
- Mustafa, I. S., Razali, N. A. N., Azman, N. Z. N., Yahaya, N. Z., Zaini, M. Z. M., Rusli, N. L., Nizamani, M. B. & Halimah, M. K. 2017. Comprehensive Study

- of Electronic Polarizability and Band Gap of  $B_2O_3$ - $Bi_2O_3$ - $ZnO$ - $SiO_2$  Glass Network. *Journal of Advanced Dielectrics*, 7(5), 1750031.
- Nandi, P. & Jose, G. 2006. Spectroscopic Properties of  $Er^{3+}$  Doped Phospho-tellurite Glasses. *Physica B: Condensed Matter*, 381(1-2), 66-72.
- Nazabal, V., Todoroki, S., Nukui, A., Matsumoto, T., Suehara, S., Hondo, T., Araki, T., Inoue, S., Rivero, C. & Cardinal, T. 2003. Oxyfluoride Tellurite Glasses Doped by Erbium: Thermal Analysis, Structural Organization and Spectral Properties. *Journal of Non-Crystalline Solids*, 325(1-3), 85-102.
- Newbury, D. E. & Ritchie, N. W. M. 2013. Is Scanning Electron Microscopy/Energy-Dispersive X-ray Spectrometry (SEM/EDS) Quantitative? *Scanning*, 35(3), 141-168.
- Newbury, D. E. & Ritchie, N. W. M. 2015. Performing Elemental Microanalysis with High Accuracy and High Precision by Scanning Electron Microscopy/Silicon Drift Detector Energy-dispersive X-ray Spectrometry (SEM-SDD-EDS). *Journal of Materials Science*, 50(2), 493-518.
- Nurhafizah, H., Rohani, M.S. & Ghoshal, S.K. 2017. Self Cleanliness of  $Er^{3+}/Nd^{3+}$  Co-doped Lithium Niobate Tellurite Glass Containing Silver Nanoparticles. *Journal of Non-Crystalline Solids*, 455, 62-69.
- O'Donnell, M. D., Miller, C. A., Furniss, D., Tikhomirov, V. K. & Seddon, A. B. 2003. Fluorotellurite Glasses with Improved Mid-infrared Transmission. *Journal of Non-Crystalline Solids*, 331(1-3), 48-57.
- Oo, H. M., Mohamed-Kamari, H., Mohd Daud Wan-Yusoff, W. 2012. Optical Properties of Bismuth Tellurite Based Glass. *International Journal of Molecular Sciences*, 13(4), 4623-4631.
- Oxford Instruments Analytical Limited. 2008. *X-Max: The Largest SDD - Size It Matters*. High Wycombe, UK: Oxford Instruments. Retrieved from <https://aiim.uow.edu.au/content/groups/public/@web/@aiim/documents/doc/uow154676.pdf> on 10 June 2018.
- Oxford Instruments Analytical Limited. 2012. *Silicon Drift Detectors Explained*. High Wycombe, UK: Oxford Instruments. Retrieved from <https://nano.oxinst.com/products/x-max/x-max> on 10 June 2018.
- Pan, Z., Ueda, A., Aga Jr., R. Burger, A., Mu, R. & Morgan, S. H. 2010. Spectroscopic Studies of  $Er^{3+}$  Doped Ge-Ga-S Glass Containing Silver Nanoparticles. *Journal of Non-Crystalline Solids*, 356(23-24), 1097-1101.
- Parveen, N., Jali, V. M. & Patil, S. D. 2016. Structure and Optical Properties of  $TeO_2$ - $GeO_2$  Glasses. *International Journal of Advances in Science Engineering and Technology*, 4(1), 89-94. Retrieved from [http://iraj.in/journal/IJASEAT/paper\\_detail.php?paper\\_id=3867&name=Structure\\_And\\_Optical\\_Properties\\_Of\\_Teo2-Geo2\\_Glasses](http://iraj.in/journal/IJASEAT/paper_detail.php?paper_id=3867&name=Structure_And_Optical_Properties_Of_Teo2-Geo2_Glasses) on 20 May 2018.

- Pavani, P.G., Sadhana, K. & Mouli, V.C. 2011. Optical, Physical and Structural Studies of Boro-zinc Tellurite Glasses. *Physica B*, 406(6-7), 1242-1247.
- Perkins, S. T., Cullen, D. E., Chen, M. H., Hubbell, J. H., Rathkopf, J. & Scofield, J. 1991. *Tables and Graphs of Atomic Subshell and Relaxation Data Derived from the LLNL Evaluated Atomic Data Library (EADL), Z = 1 – 100*. Report No. UCRL-50400-Vol. 30. Oak Ridge, USA: Office of Scientific and Technical Information. Retrieved from <https://www.osti.gov/biblio/10121422-tables-graphs-atomic-subshell-relaxation-data-derived-from-llnl-evaluated-atomic-data-library-eadl> on 20 June 2018.
- Pellerin, N., Blondeau, J-P., Noui, S., Allix, M., Ory, S., Veron, O., De Sousa Meneses, D. & Massiot. Control of Selective Silicate Glass Coloration by Gold Metallic Nanoparticles: Structural Investigation, Growth Mechanisms, and Plasmon Resonance Modelization. *Gold Bulletin*, 46(4), 243-255.
- Poppe, L.J., Paskevich, V.F., Hathaway, J.C. & Blackwood, D.S. 2001. *A Laboratory Manual for X-Ray Powder Diffraction*. Report 01-041. Woods Hole, MA: U.S. Geological Survey. Retrieved from [https://www.researchgate.net/publication/265108796\\_A\\_Laboratory\\_Manual\\_for\\_X-Ray\\_Powder\\_Diffraction](https://www.researchgate.net/publication/265108796_A_Laboratory_Manual_for_X-Ray_Powder_Diffraction) on 20 May 2018.
- Postek, M. T., Vladár, A. E. & Purushotham, K. P. 2014. Does Your SEM Really Tell the Truth? How Would You Know? Part 2. *Scanning*, 36(3), 347-355.
- Pyrz, W. D. & Buttrey, D. J. 2008. Particle Size Determination using TEM: A Discussion of Image Acquisition and Analysis for the Novice Microscopist. *Langmuir*, 24(20), 11350-11360.
- Quorum Technologies Limited Company. no yr. *Q150T Turbomolecular-pumped Coating System: High Vacuum Sputtering, Carbon and Metal Evaporation for SEM, TEM and Thin Film Applications*. East Sussex, England: Quorum Technologies. Retrieved from [https://www.quorumtech.com/\\_\\_assets\\_\\_/pdf/product/Q150T-brochure-final.pdf](https://www.quorumtech.com/__assets__/pdf/product/Q150T-brochure-final.pdf) on 20 May 2018.
- Ramer, G. & Lendl, B. 2013. Attenuated Total Reflection Fourier Transform Infrared Spectroscopy. *In Encyclopedia of Analytical Chemistry: Applications, Theory and Instrumentation*, pp. 1-27. Retrieved from <https://onlinelibrary.wiley.com/doi/abs/10.1002/9780470027318.a9287> on 20 May 2018.
- Reisfeld, R., Katz, G., Spector, N., Jørgensen, C. K., Jacobani, C. & de Pape, R. 1982. Optical Transition Probabilities of Er<sup>3+</sup> in Fluoride Glasses. *Journal of Solid State Chemistry*, 41(3), 253-261.
- Rivera, V. A. G., Osorio, S. P. A., Ledemi, Y., Manzani, D., Messadeq, Y., Nunes, L.A.O. & Marega Jr., E. 2010. Localized Surface Plasmon Resonance

- Interaction with Er<sup>3+</sup>-doped Tellurite Glass. *Optics Express*, 18(24), 25321-25328.
- Rivera, V. A. G., Manzani, D., Messaddeq, Y., Nunes, L. A. O. & Marega Jr., E. 2011. Study of Er<sup>3+</sup> Fluorescence on Tellurite Glasses Containing Ag Nanoparticles. *Journal of Physics: Conference Series*, 274(1), 012123.
- Rivera, V.A.G., Ferri, F.A. & Marega Jr, E. 2012. Localized Surface Plasmon Resonances: Noble Metal Nanoparticle Interaction with Rare-earth Ions. In K. Y. Kim (ed.). *Plasmonics - Principles and Applications*, pp. 283-312. Rijeka, Croatia: InTech. doi: 10.5772/50753. Retrieved from <https://www.intechopen.com/books/plasmonics-principles-and-applications/localized-surface-plasmon-resonances-noble-metal-nanoparticle-interaction-with-rare-earth-ions> on 20 May 2018.
- Rivera, V. A. G., Ledemi, Y., Osorio, S. P. A., Manzani, D., Ferri, F. A., Ribeiro, S. J.L., Nunes, L. A. O. & Marega Jr., E. 2013. Tunable Plasmon Resonance Modes on Gold Nanoparticles in Er<sup>3+</sup>-doped Germanium-tellurite Glass. *Journal of Non-Crystalline Solids*, 378, 126-134.
- Rivera, V. A. G., Ledemi, Y., Pereira-da-Silva, M. A., Messaddeq, Y., & Marega Jr, E. 2016. Plasmon-photon Conversion to Near-infrared Emission from Yb<sup>3+</sup>: (Au/Ag-nanoparticles) in Tungsten-tellurite Glasses. *Scientific Reports*, 6, 18464.
- Roy, B., Jain, H., Saha, S.K. & Chakravorty, D. 1995. Comparison of Structure of Alkali Silicate Glasses Prepared by Sol-gel and Melt-quench Methods. *Journal of Non-Crystalline Solids*, 183(3), 268-276.
- Ru, E. L. C. & Etchegoin, P. G. 2009a. A Quick Overview of Surface-enhanced Raman Spectroscopy. In *Principles of Surface-enhanced Raman Spectroscopy and Related Plasmonic Effects 1<sup>st</sup> Edition*, pp. 1-3. Amsterdam, The Netherlands: Elsevier. Retrieved from <http://www.fulviofrisone.com/attachments/article/406/principles%20of%20surface%20enhanced%20raman%20spectroscopy0444527796.pdf> on 20 April 2018.
- Ru, E. L. C. & Etchegoin, P. G. 2009b. EM Enhancements and Plasmon Resonances: Examples and Discussion. In *Principles of Surface-enhanced Raman Spectroscopy and Related Plasmonic Effects 1<sup>st</sup> Edition*, pp. 348. Amsterdam, The Netherlands: Elsevier. Retrieved from <http://www.fulviofrisone.com/attachments/article/406/principles%20of%20surface%20enhanced%20raman%20spectroscopy0444527796.pdf> on 20 April 2018.
- Sahar, M. R. & Ghoshal, S. K. 2015. Nanoglass: Present Challenges and Future Promises. *Advanced Materials Research*, 1108, 45-58. doi:10.4028/www.scientific.net/AMR.1108.45

- Sakka, S. 2014. Sol-gel Glasses and Their Future Applications. *Transaction of the Indian Ceramic Society*, 46(1), 1-11. doi: 10.1080/0371750X.1987.10822820
- Sangwarantee, N., Kaewkhao, J., & Chanthima, N. 2016. Visible Luminescence Properties of Sm<sup>3+</sup> Doped Magnesium Bismuth Phosphate Glasses. *Key Engineering Materials*, 675-676, 405-408.
- Selvaraju, K. & Marimuthu, K. 2012. Structural and Spectroscopic Studies on Concentration Dependent Er<sup>3+</sup> Doped Boro-tellurite Glasses. *Journal of Luminescence*, 132(5), 1171-1178.
- Selvaraju, K., Vijaya, N., Marimuthu, K. & Lavin, V. 2013. Composition Dependent Spectroscopic Properties of Er<sup>3+</sup>-doped Boro-tellurite Glasses. *Physica Status Solidi A*, 210(3), 607-615.
- Shirley, G.Z. 2014, August, 26. Need help on lognormal function fitting [Online forum post]. Message posted to [https://www.originlab.com/forum/topic.asp?TOPIC\\_ID=19913](https://www.originlab.com/forum/topic.asp?TOPIC_ID=19913)
- Shelby, J.E. 2005. Introduction. *In Introduction to Glass Science and Technology 2<sup>nd</sup> Edition*, pp. 1-3. Cambridge, UK: The Royal Society of Chemistry.
- Shelby, J.E. 2005. Glass Melting. *In Introduction to Glass Science and Technology 2<sup>nd</sup> Edition*, pp. 26-48. Cambridge, UK: The Royal Society of Chemistry.
- Sidek, H.A.A., Rosmawati, S., Talib, Z.A., Halimah, M.K. & Daud, W.M. 2009. Synthesis and Optical Properties of ZnO-TeO<sub>2</sub> Glass System. *American Journal of Applied Sciences*, 6(8), 1489-1494.
- Smith, E. and Dent, G. 2005. Introduction, Basic Theory and Principles. *In Modern Raman Spectroscopy – A Practical Approach*, pp. 1-4. West Sussex, England: John Wiley & Sons.
- Smith, B. C. 2011a. Introduction to Infrared Spectroscopy. *In Fundamentals of Fourier Transform Infrared Spectroscopy 2<sup>nd</sup> Edition*, pp. 5-6. Boca Raton, FL: CRC Press.
- Smith, B. C. 2011b. How an FTIR Works. *In Fundamentals of Fourier Transform Infrared Spectroscopy 2<sup>nd</sup> Edition*, pp. 19-27. Boca Raton, FL: CRC Press.
- Smith, B. C. 2011c. Preparing Samples Properly. *In Fundamentals of Fourier Transform Infrared Spectroscopy 2<sup>nd</sup> Edition*, pp. 129-144. Boca Raton, FL: CRC Press.
- Solé, J. G., Bausa, L.E. & Jaque, D. 2005a. Fundamentals. *In An Introduction to Optical Spectroscopy of Inorganic Solids*, pp. 8-15. West Sussex, England: John Wiley & Sons.



- Solé, J. G., Bausá, L.E. & Jaque, D. 2005b. Fundamentals. *In An Introduction to Optical Spectroscopy of Inorganic Solids*, pp. 16-18. West Sussex, England: John Wiley & Sons.
- Solé, J. G., Bausá, L.E. & Jaque, D. 2005c. Applications: Rare Earth and Transition Metal Ions, and Color Centers. *In An Introduction to Optical Spectroscopy of Inorganic Solids*, pp. 200-201. West Sussex, England: John Wiley & Sons.
- Soltani, I., Hraiech, S., Horchani-Naifer, K., Elhouichet, H., Gelloz, B. & Férid, M. 2016. Growth of Silver Nanoparticles Stimulate Spectroscopic Properties of Er<sup>3+</sup>-doped Phosphate Glasses: Heat Treatment Effect. *Journal of Alloys and Compounds*, 686, 556-563.
- Som, T. & Karmakar, B. 2008. Infrared-to-red Upconversion Luminescence in Samarium-doped Antimony Glasses. *Journal of Luminescence*, 128(12), 1989-1996.
- Som, T. & Karmakar, B. 2009a. Nanosilver Enhanced Upconversion Fluorescence of Erbium Ions in Er<sup>3+</sup>: Ag-antimony Glass Nanocomposites. *Journal of Applied Physics*, 105(1), 013102.
- Som, T. & Karmakar, B. 2009b. Enhancement of Er<sup>3+</sup> Upconverted Luminescence in Er<sup>3+</sup>: Au-antimony Glass Dichroic Nanocomposites Containing Hexagonal Au Nanoparticles. *Journal of the Optical Society of America B*, 26(12), B21-B27.
- Som, T. & Karmakar, B. 2009c. Core-shell Au-Ag Nanoparticles in Dielectric Nanocomposites with Plasmon-enhanced Fluorescence: A New Paradigm in Antimony Glasses. *Nano Research*, 2(8), 607-616.
- Som, T. & Karmakar, B. 2009d. Efficient Green and Red Fluorescence Upconversion in Erbium Doped New Low Phonon Antimony Glasses. *Optical Materials*, 31(4), 609-618.
- Som, T. & Karmakar, B. 2010a. Surface Plasmon Resonance and Enhanced Fluorescence Application of Single-step Synthesized Elliptical Nano Gold-embedded Antimony Glass Dichroic Nanocomposites. *Plasmonics*, 5(2), 149-159.
- Som, T. & Karmakar, B. 2010b. Enhanced Frequency Upconversion of Sm<sup>3+</sup> Ions by Elliptical Au Nanoparticles in Dichroic Sm<sup>3+</sup>: Au-antimony Glass Nanocomposites. *Spectrochimica Acta Part A: Molecular and Biomolecular Spectroscopy*, 75(2), 640-646.
- Som, T. & Karmakar, B. 2011. Nano Silver: Antimony Glass Hybrid Nanocomposites and Their Enhanced Fluorescence Application. *Solid State Sciences*, 13(5), 887-895.
- Som, T., Singh, S. P. & Karmakar, B. 2016. Plasmonic Antimony and Bismuth Oxide Glass: Synthesis and Enhanced Photoluminescence. *In B. Karmakar, K. Rademann & A. L. Stepanov (eds.). Glass Nanocomposites: Synthesis, Properties and Applications 1<sup>st</sup> Edition*, pp.225. Cambridge, MA: Elsevier.

- Statham, P. J. 2002. Limitations to Accuracy in Extracting Characteristic Line Intensities from X-ray Spectra. *Journal of Research of the National Institute of Standards and Technology*, 107(6), 531-546.
- Studenyyak, I., Kranjčec, M. & Kurik, M. 2014. Urbach Rule in Solid State Physics. *International Journal of Optics and Applications*, 4(3), 76-83.
- Sur, U. K. 2017. Surface-enhanced Raman scattering, Raman Spectroscopy and Applications. In K. Maaz (ed.). *Raman Spectroscopy and Applications*, pp. 293-295. Rijeka, Croatia: InTech. doi: 10.5772/66084. Retrieved from <https://www.intechopen.com/books/raman-spectroscopy-and-applications/surface-enhanced-raman-scattering> on 10 April 2019.
- Suryanarayana, C. & Norton, M. G. 1998a. Lattices and Crystal Structures. In *X-ray Diffraction: A Practical Approach 1<sup>st</sup> Edition*, pp. 60-61. New York, NY: Springer.
- Suryanarayana, C. & Norton, M. G. 1998b. Lattices and Crystal Structures. In *X-ray Diffraction: A Practical Approach 1<sup>st</sup> Edition*, pp. 50-62. New York, NY: Springer.
- Tarafder, A. 2015. *Processing and Characterization of Au<sup>0</sup> and Au<sup>0</sup>-Er<sup>3+</sup> Containing Plasmonic Glass Nanocomposites in K<sub>2</sub>O-ZnO-SiO<sub>2</sub> Glass System*. (PhD thesis). Retrieved from [http://shodhganga.inflibnet.ac.in/bitstream/10603/163894/17/17\\_chapter%208.pdf](http://shodhganga.inflibnet.ac.in/bitstream/10603/163894/17/17_chapter%208.pdf) on 20 June 2018.
- Thanh, N. T. K., Madean, N. & Mahiddine, S. 2014. Mechanisms of Nucleation and Growth of Nanoparticles in Solution. *Chemical Reviews*, 114(15), 7610-7630.
- Triola, M. F. 2010. Statistics for Describing, Exploring and Comparing Data. In *Elementary Statistics Technology Update 11<sup>th</sup> Edition*, pp. 92. Boston, MA: Pearson.
- Van Deun, R., Binnemans, K., Görller-Warland, C. & Adam, J.L. 1999. Spectroscopic Properties of Trivalent Samarium Ions in Glasses. *Proceedings Volume 3622, Rare-Earth-Doped Materials and Devices III*. January, 1999. San Jose, California. Retrieved from [https://www.researchgate.net/profile/Rik\\_Deun/publication/230687749\\_Spectroscopic\\_properties\\_of\\_trivalent\\_samarium\\_ions\\_in\\_glasses/links/0c9605168445260b99000000/Spectroscopic-properties-of-trivalent-samarium-ions-in-glasses.pdf](https://www.researchgate.net/profile/Rik_Deun/publication/230687749_Spectroscopic_properties_of_trivalent_samarium_ions_in_glasses/links/0c9605168445260b99000000/Spectroscopic-properties-of-trivalent-samarium-ions-in-glasses.pdf) on 26 June 2019.
- Vijayakumar, R. & Marimuthu, K. 2016. Luminescence Studies on Ag Nanoparticles Embedded Eu<sup>3+</sup> Doped Boro-phosphate Glasses. *Journal of Alloys and Compounds*, 665, 294-303.

- Voorhess, P. W. 1985. The Theory of Ostwald Ripening. *Journal of Statistical Physics*, 38(1-2), 231-252.
- Wang, Z. L. no yr. *Fundamental Theory of Transmission Electron Microscope*. Retrieved from <http://www.nanoscience.gatech.edu/zlwang/research/tem.html> on 10 April 2018.
- Wang, J.S., Vogel, E.M. & Snitzer, E. 1994. Tellurite Glass: A New Candidate for Fiber Devices. *Optical Materials*, 3(3), 187-203.
- Wang, Y., Deng, J., Di, J. & Tu, Y. 2009. Electrodeposition of Large Size Gold Nanoparticles on Indium Tin Oxide Glass and Application as Refractive Index Sensor. *Electrochemistry Communications*, 11(5), 1034-1037.
- Wang, C., Singh, P., Kim, Y. J., Mathiyalagan, R., Myagmarjav, D., Wang, D., Jin, C. & Yang, D. C. 2015. Characterization and Antimicrobial Application of Biosynthesized Gold and Silver Nanoparticles by using *Microbacterium resistens*. *Artificial Cells, Nanomedicine, and Biotechnology*, 44(7), 1714-1721.
- Warren, B. E. 1940. X-ray Diffraction Study of the Structure of Glass. *Chemical Reviews*, 26(2), 237-255.
- Wassilkowska, A., Czaplicka-Kotas, A., Bielski, A. & Zielina, M. 2014. An Analysis of the Elemental Composition of Micro-samples using EDS Technique. *Czasopismo Techniczne, Chemia Zeszyt 1-Ch* (18) 2014, 133-148.
- Williams, D. B. & Carter, C. B. 2009a. The Transmission Electron Microscope. In *Transmission Electron Microscopy: A Textbook for Materials Science*, pp. 3-4. New York, NY: Springer.
- Williams, D. B. & Carter, C. B. 2009b. The Transmission Electron Microscope. In *Transmission Electron Microscopy: A Textbook for Materials Science*, pp. 5-14. New York, NY: Springer.
- Williams, D. B. & Carter, C. B. 2009c. Scattering and Diffraction. In *Transmission Electron Microscopy: A Textbook for Materials Science*, pp. 24-26. New York, NY: Springer.
- Xu, H. & Jiang, Z. 2003. Dynamics of Visible-to-ultraviolet Upconversion in  $\text{YAlO}_3$ : 1%  $\text{Er}^{3+}$ . *Chemical Physics*, 287(1-2), 155-159.
- Yang, J., Zhang, L., Wen, L. Dai, S., Hu, L. & Jiang, Z. 2004. Optical Transitions and Upconversion Luminescence of  $\text{Er}^{3+}/\text{Yb}^{3+}$ -codoped Halide Modified Tellurite Glasses. *Journal of Applied Physics*, 95(6), 3020-3026.

- Yang, J., Yang, Z., Wang, Y., Qiu, J. & Song, Z. 2016. Upconversion Luminescence Enhancement of  $\text{SiO}_2:\text{Yb}^{3+}, \text{Tb}^{3+}$  Inverse Opal Photonic Crystal by Gold Nanoparticles. *Journal of Non-Crystalline Solids*, 437, 53-57.
- Yao, J. H., Elder, K. R., Guo, H. & Grant, M. 1993. Theory and Simulation of Ostwald Ripening. *Physical Review B*, 47(21), 14110-14125.
- Yen, W. M. 1986. Optical Spectroscopy of Ions in Inorganic Glasses. In I. Zschokke (ed.). *Optical Spectroscopy of Inorganic Glasses*, pp. 40-43. Dordrecht, Holland: D. Reidel Publishing Company.
- Yoko, T., Kamiya, K., Yamada, H. & Tanaka, K. 1998. Glass-forming Region and Structure of Oxyhalide Glasses in the system  $\text{LiCl-Li}_2\text{O-TeO}_2$ . *Communications of the American Ceramic Society*, 71(2), C-70 – C-71.
- Yousef, E. L. S., Hegazy, H. H., Elokr, M. M. & Aboudeif, Y. M. 2015. Raman Spectroscopy and Raman Gain Coefficient of Telluroniobium-zinc-lead Oxyglasses Doped with Rare Earth. *Chalcogenide Letters*, 12(12), 653-663. Retrieved from [http://www.chalcogen.ro/653\\_ElSayed.pdf](http://www.chalcogen.ro/653_ElSayed.pdf) on 10 May 2018.
- Yusof, N. N., Ghoshal, S. K., Ariffin, R. & Sahar, M. R. 2015. Modified Absorption Features of Titania-erbium Incorporated Plasmonic Tellurite Glass System. *Jurnal Teknologi*, 76(13), 89-94.
- Yusof, N.N., Ghoshal, S.K. & Azlan, M.N. 2017. Optical Properties of Titania Nanoparticles Embedded  $\text{Er}^{3+}$ -doped Tellurite Glass: Judd-Ofelt Analysis. *Journal of Alloys and Compounds*, 724, 1083-1092.
- Yusof, N.N., Ghoshal, S.K., Arifin, R., Awang, A., Tewari, H.S. & Hamzah, K. 2018. Self-cleaning and Spectral Attributes of Erbium-doped Sodium-zinc Tellurite Glass: Role of Titania Nanoparticles. *Journal of Non-Crystalline Solids*, 481, 225-238.
- Yusoff, N.M. & Sahar, M.R. 2015. Effect of Silver Nanoparticles Incorporated with Samarium-doped Magnesium Tellurite Glasses. *Physica B: Condensed Matter*, 456, 191-196.
- Zhang, S., Zhang, L., Liu, K., Liu, M., Yin, Y. & Gao, C. 2018. Digestive Ripening in the Formation of Monodisperse Silver Nanospheres. *Materials Chemistry Frontiers*, 2, 1328-1333.
- Zhu, M., Lei, B., Ren, F., Chen, P., Shen, Y., Guan, B., Du, Y., Li, T. & Liu, M. 2014. Branched Au Nanostructures Enriched with a Uniform Facet: Facile Synthesis and Catalytic Performances. *Scientific Reports*, 4, 5259.
- Żmojda, J., Kochanowicz, M. & Dorosz, D. 2014. Low-phonon Tellurite Glass Co-doped with  $\text{Tm}^{3+}/\text{Ho}^{3+}$  Ions for Optical Fiber Technology. *Photonics Letters of Poland*, 6(2), 56-58.

- Zschornack, G. H. 2007a. Physical Fundamentals. *In Handbook of X-ray Data*, pp. 24-35. Berlin, Germany: Springer.
- Zschornack, G. H. 2007b. X-ray Emission Lines and Atomic Level Characteristics. *In Handbook of X-ray Data*, pp. 179-486. Berlin, Germany: Springer.
- Zschornack, G. H. 2007c. Periodic Table of the Elements. *In Handbook of X-ray Data*. Berlin, Germany: Springer.